SMA Newsletter

Submillimeter Array Newsletter | Number 26 | July 2018

CONTENTS

FROM THE DIRECTOR

Dear SMA Newsletter readers,

As many readers will know, we are engaged in a major upgrade program, the wSMA, which will dramatically increase the SMA's bandwidth, polarimetry capability, and operational efficiency and reliability. Interested readers can find the white paper outlining the science case for the wSMA as SMA Memo 165 *(https://www.cfa.harvard.edu/sma/memos/165.pdf)*. During the past two years, we have conducted a number of engineering studies in support of the wSMA, and have completed the design and prototyping of several critical components and subsystems.

We recently took a major step towards making the wSMA a reality by awarding the first of a series of major contracts; this one to High Precision Devices, Inc. Under the terms of this contract, HPD, working from a conceptual design developed in the Receiver Lab, will produce the detailed design, then build and test two prototype cryostat systems including blank receiver cartridges to be delivered to SAO next year. We held a kick off meeting with HPD at the end of June, and agreed on a timetable for preliminary- and critical- design reviews, and for the delivery of the prototypes and post-delivery acceptance tests. This represents a large investment, and a huge step forward for the wSMA. This work, along with plans for other upgrades to enable the wSMA will be presented to the SMA's External Advisory Committee meeting for review later this month.

Ray Blundell

ON THE DETECTION OF A DUSTY STAR-FORMING GALAXY IN THE EARLY UNIVERSE AT Z=6

Jorge A. Zavala[1], Min S. Yun[2], David H. Hughes[3], David Wilner[4], R. J. Ivison[5,6], Alfredo Montaña[7], Elisabetta Valiante[8], Justin Spilker[1], Itziar Aretxaga[3], Stephen Eales[8], Vladimir Avila-Reese[9],Miguel Chávez[3], Asantha Cooray[10], Helmut Dannerbauer[11,12], James S. Dunlop[6], Loretta Dunne[6,8], Arturo I. Gómez-Ruiz[7], Michał J. Michałowski[13], Gopal Narayanan[2], Hooshang Nayyeri[10], Ivan Oteo[6,5], Daniel Rosa González[3], David Sánchez-Argüelles[3], F. Peter Schloerb[2], Stephen Serjeant[14], Matthew W. L. Smith[8], Elena Terlevich[3], Olga Vega[3], Alan Villalba[3], Paul van der Werf[16], Grant W. Wilson[2] and Milagros Zeballos[3]

The discovery of a population of high-redshift dusty star-forming galaxies through the opening of the submillimeter and millimeter wavelength windows (e.g. Smail et al. 1997; Barger et al. 1998; Hughes et al. 1998) continues to have a profound impact on our understanding of galaxy formation and evolution. These submillimeter-selected galaxies (SMGs), which are characterized by large star formation rates, contribute significantly to the total cosmic star formation rate density and to the cosmic infrared background. These galaxies have also been associated with the formation of proto-clusters and are considered to be the progenitors of local massive elliptical galaxies (see review by Casey et al. 2014). However, our knowledge of the physical properties of these galaxies and the prevalence of dust-obscured star formation at earlier epochs is completely unconstrained due to the lack of large samples of distant dusty star-forming galaxies.

The largest (sub-)millimeter surveys, such as those carried out by Herschel, Planck, and the South Pole Telescope, are only sensitive to the most luminous galaxies. Despite the negative *k*-correction in the (sub-)millimeter bands that leads to no significant loss of sensitivity to z ~ 10, only a handful among the hundreds of thousands of SMGs discovered thus far have been confirmed to lie at z > 5 (e.g. Capak et al. 2011; Riechers et al. 2013; Strandet et al. 2017). All of these sources are rare examples of extreme starburst galaxies with star formation rates of more than a thousand solar masses per year. In a recent paper published in Nature Astronomy (Zavala et al. 2018), the spectroscopic detection of an amplified dusty star-forming galaxy at z=6.0 with an intrinsic less-extreme SFR of ~400 $M_{\odot}$/yr is reported. The spectroscopic redshift and physical characterization of this galaxy were achieved through observations taken with the Submillimeter Array (SMA), the Large Millimeter Telescope (LMT), and the Atacama Large Millimeter/submillimeter Array (ALMA).

The galaxy named G09 83808 (also known as HATLAS J090045.4 +004125) was first identified in the Herschel ATLAS survey (Valiante et al. 2016) within the GAMA 09 hrs field and followed up with other telescopes due to its unusually ultra-red far-infrared colors, which were consistent with thermal dust emission redshifted to z > 4. The spectroscopic detections of CO and H_2O with the LMT yielded a spectroscopic redshift of z=6.0269 ± 0.0006, allowing a subsequent detection of [CII] with the SMA, as shown in **Figure 1**. This is one of the most distant galaxies ever detected with these telescopes, whose light was emitted when the Universe was just 900 million years old or 7% of its current age.

The high-angular resolution continuum observations taken with ALMA revealed an Einstein ring-like structure around a foreground galaxy at z = 0.77, implying strong gravitational galaxy-galaxy lensing (see **Figure 2**). The best-fit lens model predicts

[1]Department of Astronomy, The University of Texas at Austin, 2515 Speedway Boulevard, Austin, TX 78712, USA.; [2]Department of Astronomy, University of Massachusetts, Amherst, MA 01003, USA.; [3]Instituto Nacional de Astrofísica, Óptica y Electrónica, Luis Enrique Erro 1, 72840 Puebla, Mexico.; [4]Harvard-Smithsonian Center for Astrophysics, 60 Garden Street, Cambridge, MA 02138, USA.; [5]European Southern Observatory, Karl Schwarzschild Strasse 2, Garching bei München 85748, Germany.; [6]Institute for Astronomy, University of Edinburgh, Royal Observatory, Blackford Hill, Edinburgh EH9 3HJ, UK.; [7]Consejo Nacional de Ciencia y Tecnología—Instituto Nacional de Astrofísica, Óptica y Electrónica, Luis Enrique Erro 1, 72840 Puebla, Mexico.; [8]School of Physics and Astronomy, Cardiff University, The Parade, Cardiff CF24 3AA, UK.; [9]Instituto de Astronomía, Universidad Nacional Autónoma de México, Ciudad Universitaria, 04510 CDMX, Mexico.; [10]Department of Physics and Astronomy, University of California, Irvine, CA 92697, USA.; [11]Instituto de Astrofísica de Canarias, E-38205 La Laguna, Tenerife, Spain.; [12]Universidad de La Laguna, Departamento de Astrofísica, E-38206 La Laguna, Tenerife, Spain.; [13]Astronomical Observatory Institute, Faculty of Physics, Adam Mickiewicz University, Słoneczna 36, 60-286 Poznan, Poland.; [14]Department of Physical Sciences, The Open University, Milton Keynes MK7 6AA, UK.; [16]Leiden Observatory, Leiden University, PO Box 9513, NL-2300 RA Leiden, The Netherlands

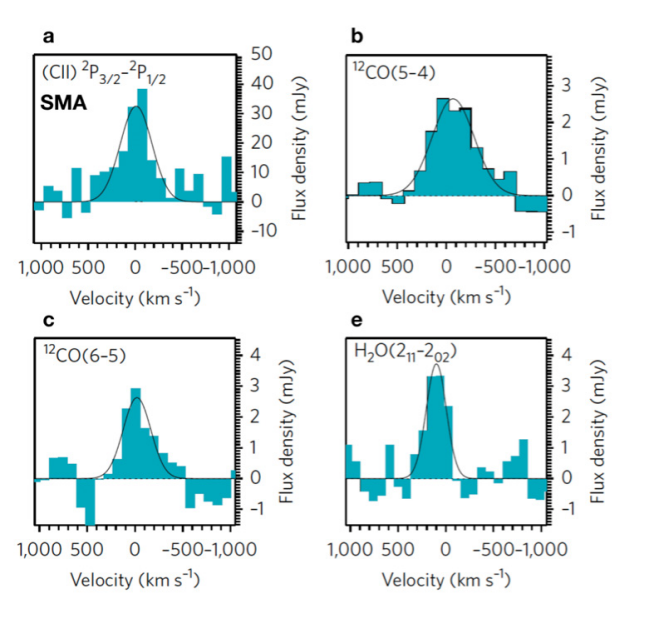

Figure 1: Emission lines detected with S/N>5 with the SMA and the LMT towards G09 83808. These transitions correspond to [CII], CO(5-4), CO(6-5), and H20(211-202). The x axis is in velocity offset with respect to the derived redshift of z=6.0269 ± 0.0006. *Figure adapted from Zavala et al. 2018.*.

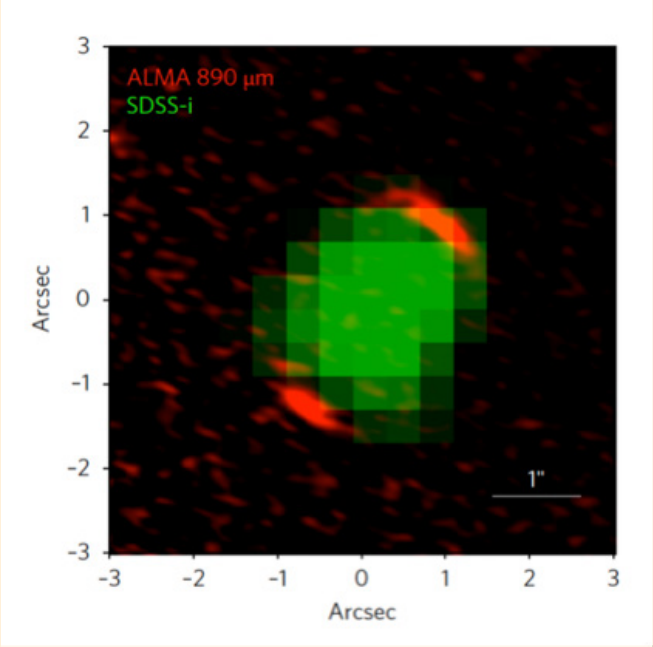

Figure 2: Color composite image of G09 83808. An Einstein ring-like structure of radius ≈ 1.4 arcsec in the ALMA image (red color) is clearly seen around a foreground galaxy at z = 0.77 detected with Sloan Digital Sky Survey (green channel), from which we derive a gravitational amplification factor of μ = 9.3 ± 1.0. *Figure adapted from Zavala et al. 2018.*

a gravitational amplification of μ = 9.3 ± 1.0. Taking this into account, an intrinsic infrared luminosity of L_{IR}=3.8 ± 0.5 × 10^{12} $M_\odot$/yr was derived for G09 83808, which implies a dust-obscured SFR of 380 ± 50 $M_\odot$/yr. This makes this galaxy a member of the ultraluminous infrared galaxy (ULIRG) population (see review by Sanders & Mirabel 1996) and one of the first spectroscopically-confirmed SMGs in this luminosity range at z > 5, bridging the gap between the extreme starbursts previously discovered at these wavelengths and the ultraviolet/optical selected star-forming galaxies with SFRs of a few dozens solar masses per year.

Surprisingly, the physical properties of G09 83808 are similar to those measured for local ULIRGs, despite a ~12.8 Gyr difference in cosmic time. This includes not only the infrared luminosity but also the dust temperature (T_D = 49 ± 3 K) and half-light radius ($R_{1/2}$ = 0.6 ± 0.1 kpc). This galaxy also follows the L'_{CO}– L_{IR} relation found for lower redshift SMGs and local ULIRGs, which is a proxy for the star formation efficiency in terms of the luminosity due to star formation and the gas content.

Although larger samples are needed to statistically characterize the star formation in the early Universe, the existence of this galaxy sheds light on our understanding of the physical properties of the first galaxies and their evolutionary path. The properties of this galaxy actually suggest that the star formation activity in these dusty star-forming galaxies has been driven by similar physical processes since the epoch of reionization.

REFERENCES

- Barger, A. et al. *Submillimetre-wavelength detection of dusty star-forming galaxies at high redshift.* Nature 394, 248 - 251 (1998).
- Capak, P. et al. *A massive protocluster of galaxies at a redshift of z ≈ 5.3.* Nature 470, 233–235 (2011).
- Casey, C. M., Narayanan, D., & Cooray, A. *Dusty star-forming galaxies at high redshift.* PhR 541, 45 (2014).
- Hughes, D. et al. *High-redshift star formation in the Hubble Deep Field revealed by a submillimetre-wavelength survey.* Nature 394, 241–247 (1998).
- Riechers, D. et al. *A dust-obscured massive maximum-starburst galaxy at a redshift of 6.34.* Nature 496, 329–333 (2013).
- Sanders, D. & Mirabel, I. *Luminous infrared galaxies.* Ann. Rev. Astron. Astrophys. 34, 749–792 (1996).
- Smail, I., Ivison, R. J. & Blain, *A. W. A deep sub-millimeter survey of lensing clusters: a new window on galaxy formation and evolution.* Astrophys. J. Lett. 490, L5–L8 (1997).
- Strandet, M. et al. ISM *properties of a massive dusty star-forming galaxy discovered at z ~ 7.* Astrophys. J. Lett. 842, L15 (2017).
- Valiante, E. et al. *The Herschel-ATLAS data release 1 - I. Maps, catalogues and number counts.* MNRAS 462, 3146 (2016).
- Zavala, J. et al. *A dust star-forming galaxy at z=6 revealed by strong gravitational lensing.* Nature Astronomy 2, 56 (2018).

HIGH-RESOLUTION SMA IMAGING OF BRIGHT SUBMILLIMETRE SOURCES FROM THE SCUBA-2 COSMOLOGY LEGACY SURVEY

Ryley Hill,[1] Scott C. Chapman,[2] Douglas Scott,[1] Glen Petitpas,[3] Ian Smail,[4] Edward L. Chapin,[5] Mark A. Gurwell,[3] Ryan Perry,[2] Andrew W. Blain,[6] Malcolm N. Bremer,[7] Chian-Chou Chen,[4,8] James S. Dunlop,[9] Duncan Farrah,[10] Giovanni G. Fazio,[3] James E. Geach,[11] Paul Howson,[2] R. J. Ivison,[8,9] Kevin Lacaille,[2,12] Michał J. Michałowski,[13] James M. Simpson,[9,14] A. M. Swinbank,[4] Paul P. van der Werf,[15] David J. Wilner

The emergence of submillimetre (submm) astronomy has led to the discovery of a cosmologically important population of submm galaxies (SMGs) that appear to be among the earliest and most actively star-forming galaxies in the Universe. While single-dish observations of SMGs have been able to greatly increase our knowledge about the evolution of star formation in the Universe (e.g., Magnelli et al. 2013; Gruppioni et al. 2013; Swinbank et al. 2014; Koprowski et al. 2017), there remain unanswered questions arising from the lack of resolution (typically between 10″ and 30″) at these wavelengths. How are their extreme luminosities sustained, and how important are mergers?

Fully resolving the submm emission directly was not possible until the leap in continuum sensitivity provided by new submm interferometers and wide-bandwidth correlators. However, finding the rarest and most massive SMGs that really push our models is far too time consuming and expensive with submm interferometry. To circumvent this issue, interferometers can be used to follow-up the brightest sources detected in large single-dish submm surveys (Barger et al. 2012; Smolčić et al. 2012b; Hodge et al. 2013; Simpson et al. 2015), providing substantial catalogues of resolved, ultra-luminous galaxies.

To date, the largest ground-based submm survey of the extragalactic sky is the SCUBA-2 Cosmology Legacy Survey (S2CLS; Geach et al. 2017), encompassing 5 deg^2 of the sky at 450 μm and 850 μm over seven cosmological fields. Using the Submillimeter Array (SMA), we have recently completed a follow-up campaign to resolve 70 of the brightest ($S_{850} \geqslant 10$ mJy) sources detected in five of the seven cosmological fields. We set up the SMA in the compact configuration, tuned to 860 μm with a bandwidth of at least 4 GHz, and had available between six and eight 6-m dishes for a given track. The synthesized beam achieved in this set up was on average 2.4″ full-width at half-maximum with our natural weighting of the visibilities, corresponding to about 20 kpc between redshifts 2 and 3 (the typical range of our targets; see Simpson et al. 2015), and the average rms sensitivity was 1.5 mJy/beam.

Figure 1 shows a representative sample of our (*CLEAN*ed) observations as contours of 2, 4 and 6 times the rms, overlaid on the original SCUBA-2 sources and existing Spitzer-IRAC 3.6-μm and VLA 1.4-GHz data. Overall we detected 61 submm galaxies above a 4σ depth of about 6 mJy, after taking into account flux boosting in our sample; 12 of our pointings turned out to be blank, and three of our pointings found a pair of galaxies.

Using our SMA data we can assess the importance of multiplicity in SMGs at the achieved resolution and sensitivity. It is well known that SMGs frequently break up into multiple sources in higher resolution imaging (e.g., Younger et al. 2007, 2009; Smolčić et al. 2012b; Hodge et al. 2013; Simpson et al. 2015); however, with sufficient sensitivity one might expect to see multiplicity in *all* galaxies (consider for example the Milky Way's dozen or more satellites). A *bone fide* merger, though, involves two galaxies of

[1] Department of Physics and Astronomy, University of British Columbia, 6225 Agricultural Road, Vancouver, V6T 1Z1, Canada; [2] Department of Physics and Atmospheric Science, Dalhousie University, 6310 Coburg Road, Halifax, B3H 4R2, Canada; [3]Harvard-Smithsonian Center for Astrophysics, 60 Garden Street, Cambridge, MA 02138, USA; [4] Centre for Extragalactic Astronomy, Department of Physics, Durham University, South Road, Durham, DH1 3LE, UK; [5] Herzberg Astronomy and Astrophysics, National Research Council Canada, 5071 West Saanich Road, Victoria, V9E 2E7, Canada; [6] Department of Physics and Astronomy, University of Leicester, University Road, Leicester, LE1 7RH, UK; [7] H.H. Wills Physics Laboratory, University of Bristol, Tyndall Avenue, Bristol, BS8 1TL, UK; [8] European Southern Observatory, Karl-Schwarzschild-Straße 2, Garching, 85748, Germany; [9] Institute for Astronomy, University of Edinburgh, Royal Observatory, Edinburgh, EH9 3HJ, UK; [10] Department of Physics MC 0435, Virginia Polytechnic Institute and State University, 850 West Campus Drive, Blacksburg, VA 24061, USA ; [11] Centre for Astrophysics Research, School of Physics, Astronomy and Mathematics, University of Hertfordshire, Roehyde Way, Hatfield, AL10 9AB, UK; [12] Department of Physics and Astronomy, McMaster University, 1280 Main Street West, Hamilton, L8S 4M1, Canada ; [13] Astronomical Observatory Institute, Faculty of Physics, Adam Mickiewicz University, ul. Słoneczna 36, 60-286 Poznan, Poland ; [14] Academia Sinica Institute of Astronomy and Astrophysics, No. 1, Sec. 4, Roosevelt Road, Taipei 10617, Taiwan; [15] Leiden Observatory, Leiden University, P.O. box 9513, Leiden, NL-2300 RA, the Netherlands

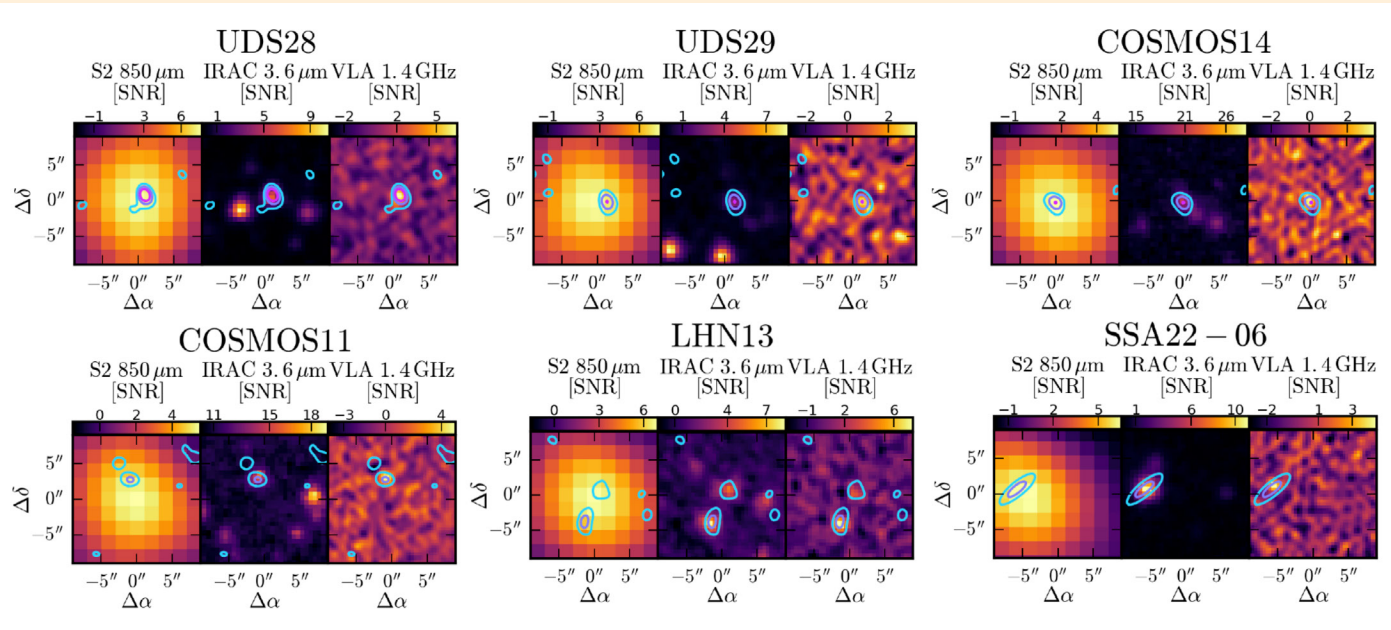

Figure 1: Multiwavelength cutouts of a representative subset of our primary beam-corrected, *CLEAN*ed images with existing Spitzer-IRAC 3.6 μm and VLA 1.4 GHz imaging. We show SMA flux contours of 2, 4 and 6 times the rms of each image overlaid over the IR and radio data, plus the parent SCUBA-2 850 μm data.

similar scale interacting within tens of parsecs of one another, and this is precisely the scenario that our data are sensitive to. If a 12-mJy SCUBA-2 source resolves into two galaxies 6 mJy each, they would be detected; if a 12-mJy SCUBA-2 source resolves into an 11-mJy galaxy and a 1-mJy galaxy, we would only observe the brightest galaxy. Indeed, the latter case is largely what we found. We estimated an upper limit of 15% for the fraction of bright (≈ 10 mJy) single dish submm sources that resolve into two or more galaxies with similar flux densities. This result suggests that most of the bright SMGs we observe are *not* significantly affected by multiplicity. We emphasize that this does not mean that there is no multiplicity in observations with higher resolution and sensitivity, we simply mean that the main components of bright SMGs are only marginally fainter than previously thought and are not undergoing a major merger with a galaxy of similar size.

These observations can be quantified in terms of number counts. **Figure 2** shows a comparison of the cumulative and differential number counts of our sample, compared to the number counts derived from two single-dish surveys (Weiß et al. 2009; Geach et al. 2017) and two previous interferometric follow-up surveys that covered much smaller sky areas (Karim et al. 2013; Simpson et al. 2015). In this plot, we have included the number counts from models of evolving star-forming galaxies, specifically the empirical model from Béthermin et al. (2012) and the GALFORM model from Lacey et al. (2016). We see no evidence for a lack of high flux-density sources, expected if most of the brightest SMGs resolved into groups of similar galaxies; instead, we see the number counts carrying on without a steep drop-off around 15 mJy.

The surface density of bright SMGs in our sample is about 8 deg^{-2}, which, assuming half of the redshifts are between 2 and 3, corresponds to a volume density of around 3×10^{-7} Mpc^{-3}. Starburst lifetimes have been estimated to be of order 100 Myr (e.g., Swinbank et al. 2006; Hainline et al. 2011; Hickox et al. 2012; Bothwell et al. 2013), and noting that z = 2–3 corresponds to a lookback time of 1 Gyr, we would expect a volume density of remnants to be approximately 3×10^{-6} Mpc^{-3}.

Local quiescent galaxies are expected to be the descendants of the starbursting galaxies in our sample (e.g., Koprowski et al. 2016; Michałowski et al. 2017; Simpson et al. 2017), and their number densities have already been measured (Bell et al. 2003; Baldry et al. 2012; Moustakas et al. 2013). So, at what stellar mass do local quiescent galaxies have the same number density as our SMGs? The answer turns out to be around 4×10^{11} $M_\odot$. Now, the typical star-formation rate (SFR) of our galaxies can be estimated assuming a standard spectral energy distribution for SMGs (Danielson et al. 2017) and using a well-known FIR luminosity-to-SFR conversion (Kennicutt 1998), which yields approximately 400 $M_\odot yr^{-1}$. This implies that about 10% of the total stellar mass assembled in our SMGs by z = 0 was produced over the 100 Myr bursts. This could be a useful test for future simulations of galaxy formation, which will need to replicate these incredibly vigorous conditions.

Our observations now provide the largest catalogue of the brightest interferometrically identified submm sources, probing the range of flux densities above 10 mJy. This catalogue is well suited for future multiwavelength follow-up studies of some of the most extreme galaxies in the Universe. Our work with the SMA also provides some of the best available submm interferometric data of several northern cosmological fields, thereby providing access to facilities in both hemispheres.

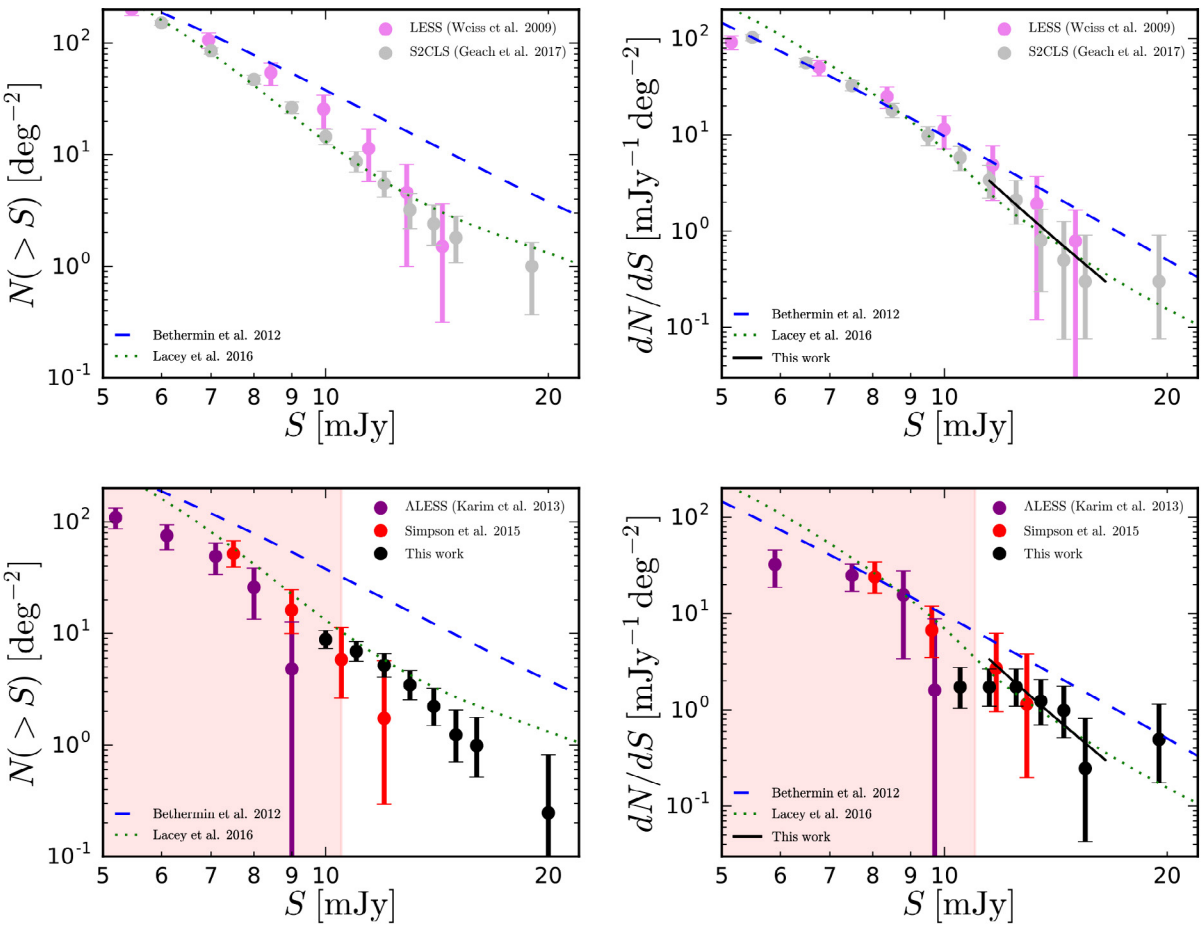

Figure 2: Cumulative and differential number counts for the two large single dish submm surveys LESS (Weiß et al. 2009) and S2CLS (Geach et al. 2017) in the top row. In the bottom row we show cumulative and differential number counts from Karim et al. (2013) and Simpson et al. (2015), interferometric follow-up studies of the LESS and S2CLS surveys, respectively, along with our SMA results. The shaded region indicates where our data are no longer 100% complete. Also shown are the models of Béthermin et al. (2012) and Lacey et al. (2016). The black solid line shows the best-fit power law to our differential distribution between 11 and 16 mJy. This plot emphasizes that number counts of the brightest SMGs are hardly affected by arcsecond-resolution imaging; instead, these ultra-bright sources are intrinsically ultra-luminous galaxies.

REFERENCES

- Baldry I. K., et al., 2012, MNRAS, 421, 621
- Barger A. J., Wang W.-H., Cowie L. L., Owen F. N., Chen C.-C., Williams J. P., 2012, ApJ, 761, 89
- Bell E. F., McIntosh D. H., Katz N., Weinberg M. D., 2003, ApJS, 149, 289
- Béthermin M., et al., 2012, ApJ, 757, L23
- Bothwell M. S., et al., 2013, MNRAS, 429, 3047
- Danielson A. L. R., et al., 2017, ApJ, 840, 78
- Geach J. E., et al., 2017, MNRAS, 465, 1789
- Gruppioni C., et al., 2013, MNRAS, 432, 23
- Hainline L. J., Blain A. W., Smail I., Alexander D. M., Armus L., Chapman S. C., Ivison R. J., 2011, ApJ, 740, 96
- Hickox R. C., et al., 2012, MNRAS, 421, 284
- Hodge J. A., et al., 2013, ApJ, 768, 91
- Karim A., et al., 2013, MNRAS, 432, 2
- Kennicutt Jr. R. C., 1998, ARA&A, 36, 189
- Koprowski M. P., et al., 2016, MNRAS, 458, 4321
- Koprowski M. P., Dunlop J. S., Michałowski M. J., Coppin K. E. K., Geach J. E., McLure R. J., Scott D., van der Werf P. P., 2017, preprint, (arXiv:1706.00426)
- Lacey C. G., et al., 2016, MNRAS, 462, 3854
- Magnelli B., et al., 2013, A&A, 553, A132
- Michałowski M. J., et al., 2017, MNRAS, 469, 492
- Moustakas J., et al., 2013, ApJ, 767, 50
- Simpson- J. M., et al., 2015, ApJ, 799, 81
- Simpson J. M., et al., 2017, ApJ, 839, 58
- Smolčić V., et al., 2012, A&A, 548, A4
- Swinbank A. M., Chapman S. C., Smail I., Lindner C., Borys C., Blain A. W., Ivison R. J., Lewis G. F., 2006, MNRAS, 371, 465
- Swinbank A. M., et al., 2014, MNRAS, 438, 1267
- Weiß A., et al., 2009, ApJ, 707, 1201
- Younger J. D., et al., 2007, ApJ, 671, 1531
- Younger J. D., et al., 2009, ApJ, 704, 803

SMA OBSERVATIONS OF POLARIZED DUST EMISSION IN SOLAR-TYPE CLASS 0 PROTOSTARS: MAGNETIC FIELD PROPERTIES AT ENVELOPE SCALES

Maud Galametz[1], Anaelle Maury[1,5], Josep M. Girart[2,3,] Ramprasad Rao[4], Qizhou Zhang[5], Mathilde Gaudel[1], Valeska Valdivia[1], Eric Keto[5], Shih-Ping Lai[6]

Magneto-hydrodynamical models have shown that the outcome of protostellar collapse can be strongly affected by the presence of magnetic fields (Galli et al. 2006; Li et al. 2014). Their role, however, still needs to be better quantified observationally. Class 0 protostars are ideal targets to study the role of these magnetic fields during the accretion processes as it is during that phase that most of the accretion occurs (André et al. 1993; André et al. 2000). Observations of the dust polarized emission is commonly used to probe the magnetic field morphology, as non-spherical dust grains align preferentially to the local magnetic field. During the last 10 years, polarization observations have been carried out in order to characterize the magnetic field topology at protostellar envelope scales (Girart et al. 2006; Rao et al. 2009; Hull et al. 2014). By comparing the large and small scale B fields of protostars at 1 mm, Hull et al. (2014) find for instance that sources with higher fractional polarizations have consistent large and small scale magnetic field orientations, which could be a signature of the regulating role of magnetic fields during the infall of the protostellar core. No systematic relation, however, has been demonstrated between the core magnetic field direction and the outflow orientation (Curran & Chrysostomou 2007; Hull et al. 2013; Zhang et al. 2014).

We obtained observations of the 0.87 mm polarized dust continuum for a sample of 12 Class 0 (single and multiple systems) protostars with the SMA interferometer. These observations give us access to the magnetic field morphology on 750-2000 au scales. The 0.87mm dust continuum maps (color scale and contours) are shown in **Fig. 1** along with the magnetic field orientation (overlaid with orange and red vectors). Those vectors are inferred from the polarization angles by applying a 90° rotation. In spite of their low luminosity, we detect linearly polarized continuum emission in all the low-mass protostars. Polarization is not always detected toward the peak of dust continuum emission. We observe a clear drop in the polarization fraction with increasing column density. This depolarization could be linked with geometrical effects (e.g. averaging effects along the line of sight or within the beam) as well as physical effects (e.g. variation in the grain alignment efficiency, grain growth, optical depth effects). Those different effects are difficult to disentangle at the resolution of our observations.

Half of the objects we analyzed have a magnetic field direction oriented within 40° of the outflow axis but some sources present strongly misaligned magnetic fields (>60° difference between B and the outflow direction). We show a histogram of the projected angles between the magnetic field orientation and the outflow direction in **Fig. 2**. The distribution looks roughly bimodal, suggesting that at the scales traced with the SMA, the B-field lines are either aligned with or perpendicular to the outflow direction. We did not find a relation between this misalignment and the polarization fraction nor intensity in our Class 0 focused sample.

Sources that show strong misalignment (close to 90°) of B with the outflow axis, such as L1448N-B or CB230, also present a clear velocity gradient perpendicular to the outflow direction. The high mass-to-flux ratio observed in these sources could favor a gravitational pull of the equatorial field lines in the main rotation plane and produce a toroidal/radial field from an initially

[1]Astrophysics department, CEA/DRF/IRFU/DAp, Université Paris Saclay, UMR AIM, F-91191 Gif-sur-Yvette, France; [2] Institut de Ciències de l'Espai (ICE, CSIC), Can Magrans, S/N, E-08193 Cerdanyola del Vallès, Catalonia, Spain; [3] Institut d'Estudis Espacials de de Catalunya (IEEC), E-08034 Barcelona, Catalonia, Spain; [4] Institute of Astronomy and Astrophysics, Academia Sinica, 645 N. Aohoku Pl., Hilo, HI 96720, USA; [5] Harvard-Smithsonian Center for Astrophysics, 60 Garden street, Cambridge, MA 02138, USA; [6] Institute of Astronomy and Department of Physics, National Tsing Hua University, Hsinchu 30013, Taiwan

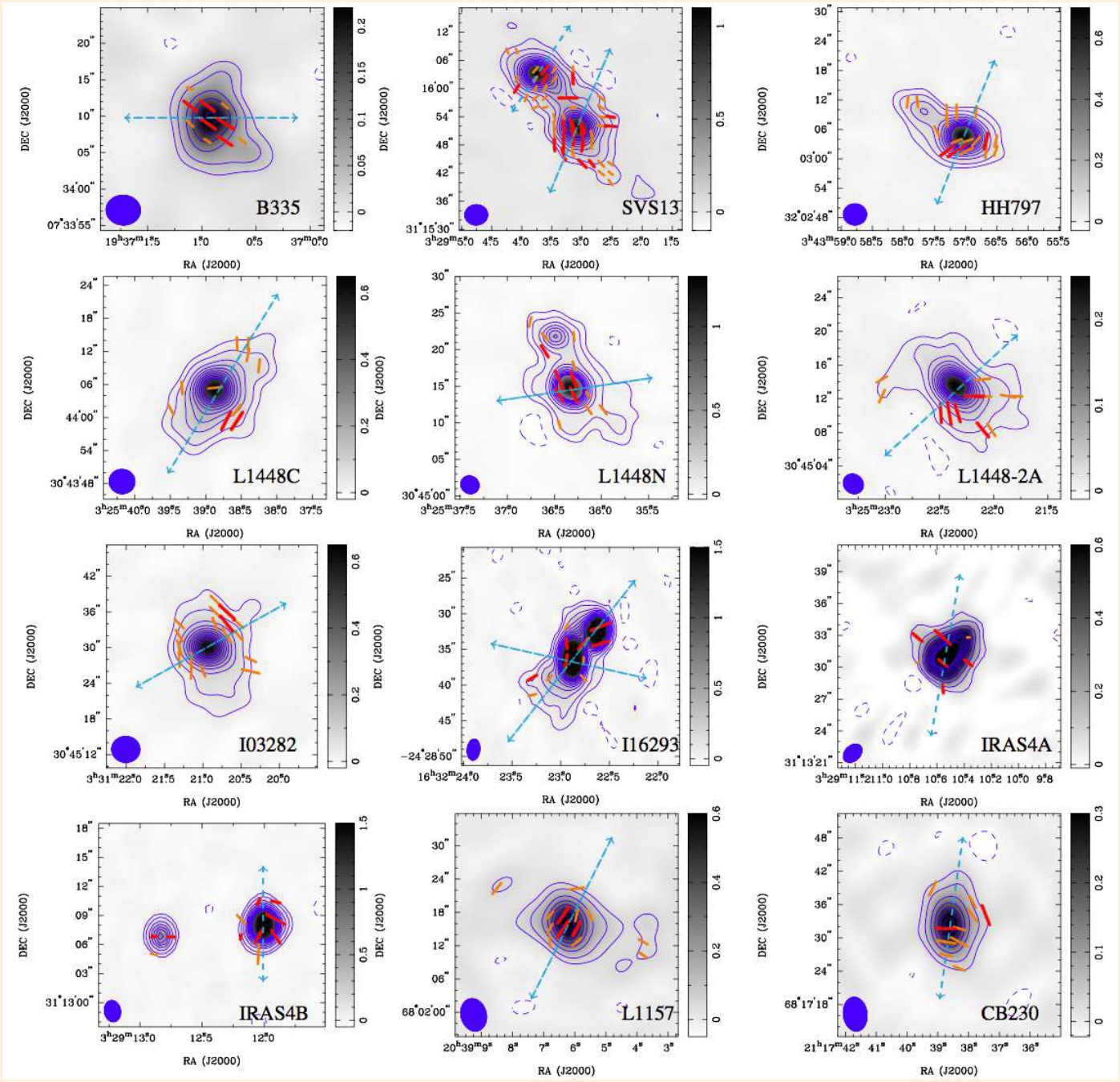

Figure 1: Map and contours: SMA 870 μm (Stokes I) dust continuum observations of a sample of 12 Class 0 protostellar envelopes. The filled ellipses in the bottom left corners indicate the synthesized beam of the SMA maps. The blue arrows indicate the outflow direction for each object. The B orientations (derived from the polarization angles assuming a 90° rotation) are overlaid on the Stokes I maps. Red bars show > 3σ detections. We also indicate the >2σ detections with orange bars but these detections were not used in the analysis.

poloidal field. The opposite causal relationship is also possible: an initially misaligned magnetic field configuration could be less efficient at braking the rotation and lead to the large rotational motions detected at envelope scales. On the contrary, we find only small misalignments in L1157 and B335, sources that show low to no velocity gradient at 1000 au scales (Tobin et al. 2011; Yen et al. 2010, Gaudel et al. in prep). The B orientation of the off-center detection in L1448C (**Fig. 1**) is also well aligned with the outflow axis and the source has one of the smallest velocity gradients perpendicular to the outflow axis determined by Yen et al. (2015). Our wide-multiple systems IRAS16293 (A and B) and SVS13 (A and B) present good alignments. In IRAS16293-A, the magnetic field has an hourglass shape at smaller scales (Rao et al. 2009), a signature of strong magnetic fields in the source. Both

sources however show a strong velocity gradient perpendicular to the outflow direction that could be responsible for some of the small tilts observed in B.

Our work suggests that the orientation of B at the envelope scales traced by the SMA can be affected by the presence of strong rotational energy in the envelope. These results are consistent with predictions from numerical simulations that show a strong relation between the angular velocity of the envelope and magnetic field direction (Machida et al. 2005; Machida et al. 2007). Reinforcing the possible correlation between the field misalignment and the presence of strong rotational motions, the SMA observations also suggest that a possible correlation could be present between the envelope-scale main magnetic field direction and the multiplicity observed in the inner envelopes. Indeed, sources that present a strong misalignment (IRAS 03282, NGC 1333 IRAS4A, L1448N, L1448-2A or CB230) are all close multiples. On the contrary, sources that show an alignment between the B direction and the outflow direction (e.g., L1157, B335, SVS13-B, and L1448C) have been studied with ALMA or NOEMA high-resolution observations and stand as robust single protostars at envelope scales of about 5000-10000 au. No large disk has been detected so far in these sources while L1448N-B for instance was suggested recently to harbor a large disk encompassing several multiple sources at scales ~100 au (Tobin et al. 2016).

These results support those of Zhang et al. (2014) that suggest a possible link between fragmentation and the magnetic field topology and point toward a less efficient magnetic braking and redistribution of angular momentum when the B-field is misaligned. They also support theoretical predictions from magnetic collapse models (Machida et al. 2005; Joos et al. 2012). More observations of the magnetic field of low-mass protostars at envelope scale would be necessary to observationally confirm these 'tentative' but promising results and re-enforce our interpretations. A similar SMA observing program will be carried out during the summer semester, allowing us to extend this analysis to a sample twice as large.

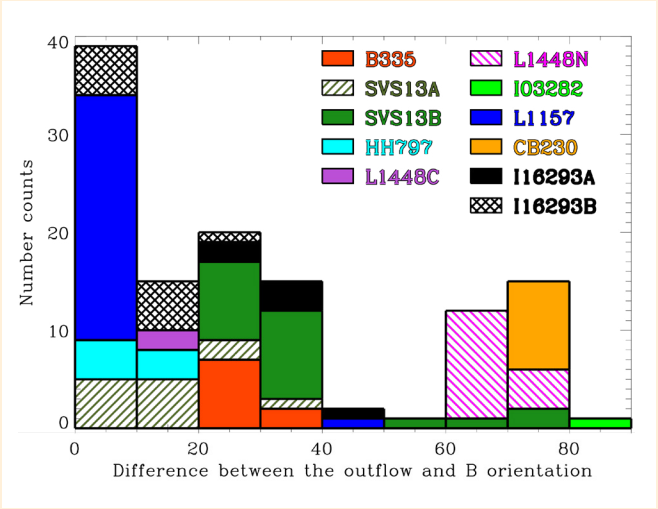

Figure 2: Histogram of the projected angles between the magnetic field orientation and the outflow direction. The SMA data are binned with pixels of 1.8''. The bimodality of the distribution shows that the B-field lines either aligned or perpendicular to the outflow direction.

REFERENCES

- André, P., Ward-Thompson, D., & Barsony, M. 1993, ApJ, 406, 122
- Andre, P., Ward-Thompson, D., & Barsony, M. 2000, Protostars and Planets IV, 59
- Chandler, C. J., Brogan, C. L., Shirley, Y. L., & Loinard, L. 2005, ApJ, 632, 371
- Chiang, H.-F., Looney, L. W., & Tobin, J. J. 2012, ApJ, 756, 168
- Choi, M. 2005, ApJ, 630, 976
- Curran, R. L. & Chrysostomou, A. 2007, MNRAS, 382, 699
- Galli, D., Lizano, S., Shu, F. H., & Allen, A. 2006, ApJ, 647, 374
- Girart, J. M., Rao, R., & Marrone, D. P. 2006, Science, 313, 812
- Hull, C. L. H., Plambeck, R. L., Bolatto, A. D., et al. 2013, ApJ, 768, 159
- Hull, C. L. H., Plambeck, R. L., Kwon, W., et al. 2014, ApJS, 213, 13
- Joos, M., Hennebelle, P., & Ciardi, A. 2012, A&A, 543, A128
- Launhardt, R. 2004, in IAU Symposium, Vol. 221, Star Formation at High Angular Resolution, ed. M. G. Burton, R. Jayawardhana, & T.L. Bourke, 213
- Li, H.-B., Goodman, A., Sridharan, T. K., et al. 2014, Protostars and Planets VI, 101
- Machida, M. N., Matsumoto, T., Tomisaka, K., & Hanawa, T. 2005, MNRAS, 362, 369
- Machida, M. N., Inutsuka, S.-i., & Matsumoto, T. 2007, ApJ, 670, 1198
- Rao, R., Girart, J. M., Marrone, D. P., Lai, S.-P., & Schnee, S. 2009, ApJ, 707, 921
- Saito, M., Sunada, K., Kawabe, R., Kitamura, Y., & Hirano, N. 1999, ApJ, 518, 334
- Tobin, J. J., Hartmann, L., Chiang, H.-F., et al. 2011, ApJ, 740, 45
- Tobin, J. J., Chandler, C. J., Wilner, D. J., et al. 2013, ApJ, 779, 93
- Tobin, J. J., Looney, L. W., Li, Z.-Y., et al. 2016, ApJ, 818, 73
- Tobin, J. J., Looney, L. W., Wilner, D. J., et al. 2015, ApJ, 805, 125
- Yen, H.-W., Takakuwa, S., & Ohashi, N. 2010, ApJ, 710, 1786
- Yen, H.-W., Koch, P. M., Takakuwa, S., et al. 2015, ApJ, 799, 193
- Zhang, Q., Qiu, K., Girart, J. M., et al. 2014, ApJ, 792, 116

STAR FORMATION IN A HIGH-PRESSURE ENVIRONMENT: AN SMA VIEW OF THE GALACTIC CENTRE DUST RIDGE

D. L. Walker[1], S. N. Longmore[2], Q. Zhang[3], C. Battersby[4], E. Keto[3], J. M. D. Kruijssen[5], A. Ginsburg[6], X. Lu[7], J. D. Henshaw[5], J. Kauffmann[8], T. Pillai[9], E. A. C. Mills[10], A. J. Walsh[11], J. Bally[12], L. C. Ho[13], K. Immer[14], K. G. Johnston[15]

Empirical star formation relations that describe the conversion from gas into stars are fundamental to astronomy. To date, such relations have largely been calibrated through detailed studies of star-forming regions in the disc of the Milky Way and nearby galaxies. However, these regions are typically very similar in terms of their environmental conditions. If we wish to apply star formation relations to the vastly differing environments that are found throughout the Universe, then it is crucial that we test their validity in regions with significantly different environmental conditions.

At a distance of 8.4 kpc (Reid et al. 2014), the Galactic centre is our nearest extreme environment. The Central Molecular Zone (CMZ, inner few hundred parsecs of the Galaxy) differs from the Galactic disc in a number of key physical and kinematic properties. These include the fact that the average gas density is at least an order of magnitude higher (e.g. Longmore et al. 2013), with high turbulent line widths (e.g. Shetty et al. 2012), a substantial fraction of hot gas (e.g. Ginsburg et al. 2016; Immer et al 2016), and heightened pressures, cosmic ray ionisation rates and magnetic field strengths (e.g. Kruijssen et al. 2014). There is also mounting evidence that the critical density threshold required for stars to form in the CMZ is substantially greater than elsewhere in the Galaxy (e.g. Longmore et al. 2013; Ginsburg et al. 2018), which may explain the fact that the current star formation rate is at least an order of magnitude lower than predicted given the amount of dense gas (e.g. Longmore et al. 2013; Barnes et al. 2017). Furthermore, the gas conditions in this environment are similar to those in high-redshift starburst galaxies (Kruijssen & Longmore 2013), and may therefore serve as a local analogue that we can study in far greater detail than is achievable at high-redshift.

In an effort to understand the nature of star formation in the CMZ, we have conducted a large-scale survey of the region with the SMA (*CMZoom*, Battersby et al. 2017). We have observed all material above a column density threshold of 10^{23} cm^{-2}, as this is where we would expect any on-going and potential sites of star formation to be found. The observations were taken at 230 GHz and with ~ 3-4" angular resolution (~ 0.1 pc at the distance of the CMZ), with both the compact and subcompact SMA configurations. To recover the zero-spacing emission, we use data from the Bolocam Galactic Plane Survey (BGPS v2.1, e.g. Rosolowsky et al. 2010) for the continuum, and data from a recent survey of the CMZ performed using the Atacama Pathfinder EXperiment (APEX) telescope for the molecular line emission (Ginsburg et al. 2016). Here, we summarise the results from Walker et al. (2018), in which we study a subset of the molecular clouds from the CMZoom survey. These clouds — G0.340+0.055, G0.380+0.050, G0.412+0.052, G0.478−0.005, and G0.496+0.020 — belong to the so-called *dust ridge*, which is a gas stream that is situated ~ 100 pc in front of the Galactic centre and spans ~ 45 pc in projected longitude. The dust ridge clouds are all high-mass (> 10^4 $M_\odot$), compact (R ~ few parsecs) and contain little-to-no widespread star formation, despite their high mean densities (~ 10^4 cm^{-3}).

Our SMA observations have revealed that, while these clouds are not highly star-forming, they do contain a large degree of dense sub-structure (see **Figure 1**). Overall, we detect 15 cores with radii ~ 0.15 pc that range in mass from 50 - 2000 $M_\odot$. Analysis of the molecular line emission reveals that the line-widths are quite large even on these scales (~ 5 km/s). Simple virial analysis comparing the kinetic energy in the gas inferred from these line-widths and the gravitational energy leads to the conclusion that

[1]NAOJ/ALMA; [2]LJMU; [3]CfA; [4]CfA; [5]Heidelberg; [6]NRAO; [7]NAOJ; [8]MIT; [9]MPIfR; [10]MPIfR; [11]ICRAR; [12]UCB; [13]Peking U.; [14]ESO; [15]Leeds

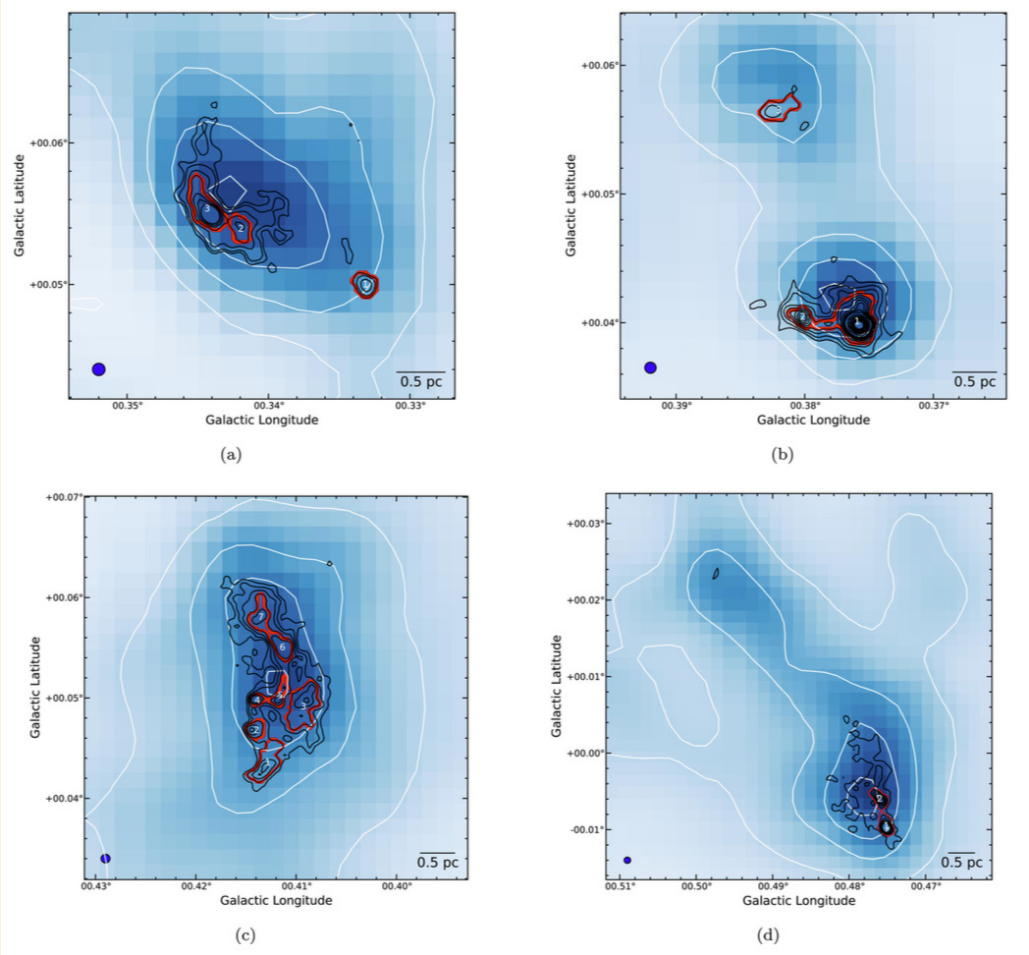

Figure 1: Top: dust ridge clouds 'G0.340+0.055' (left) and 'G0.380+0.050' (right). Bottom: dust ridge clouds 'G0.412+0.052' (left) and 'G0.478–0.005/ G0.496+0.020' (right). Background image is a Herschel column density map, shown with corresponding white contours. Black contours show the 230 GHz continuum emission as seen with the SMA at the 5σ level. They are 10–32, 16–460, 16–32 and 20–72 mJy beam^{-1} for clouds b, c, d and e/f, respectively. The synthesised beam is shown in the lower left of each panel. Red contours highlight the cores as determined via dendrogram analysis.

these cores are unlikely to be gravitationally bound. If we instead consider the case of pressure-bounded virial equilibrium, we find that pressures of $P_e/k \sim 10^8$ K cm^{-3} are required. This is consistent with the observed large-scale turbulent pressures in the CMZ (Kruijssen & Longmore 2013; Longmore et al. 2014; Rathborne et al. 2014), and so the cores may well be gravitationally-bound despite their large line-widths.

Of the 15 cores detected, we find that only two cores show signs of active star formation, as determined by searching for H_2O and CH_3OH Class II maser emission, along with 24 μm and 70 μm emission. Coupled with their masses and their rich 'hot core' molecular line emission, we conclude that these two sources are newly-discovered high-mass protostars. Additionally, there are no detections of UCHII regions towards these sources, as revealed by deep VLA observations (Immer et al. 2012). Thus, any high-mass stars forming within these sources are likely very young. Detailed studies of these protostars promise to provide unique insight into the early formation of massive stars in the CMZ. We currently have multiple follow-up projects with ALMA to observe these massive protostars on ~ 1000 AU scales.

We compare our sample of 15 high-mass cores to a sample of high-mass cores in the Galactic disc taken from the literature (Peretto et al. 2013, Louvet et al. 2014). Figure 2 shows a mass-radius plot comparing both samples. This shows that the bulk physical properties of the cores in the CMZ and the disc are indistinguishable. However, the key difference here is that *all* of the high-mass cores in the disc are actively star-forming, whereas we find that only two out of fifteen in the CMZ are, despite their high densities and the high external pressures that they are subjected to in the CMZ. This adds further evidence to the idea that the critical density threshold for star formation is elevated in this region on the Galaxy. This has important implications for the way galaxies convert their gas content to stars over cosmological timescales.

A leading theory for the heightened critical density threshold in the CMZ is that it results from the very high turbulent energy density in this region (e.g. Krumholz & McKee, 2005; Padoan & Nordlund, 2011). These models postulate that the critical density threshold is determined via $\rho_{crit} \propto P_{turb}/T_g$ — where P_{turb} is the turbulent pressure, and T_g is the gas temperature. For representative gas conditions in the Galactic disc and the CMZ, the predicted critical density thresholds vary by 3-4 orders of magnitude. The corresponding thresholds are shown in **Figure 2**. We see that all of the cores in the disc are above the appropriate threshold, which is consistent with their active star formation, whereas all of the CMZ sources are below the predicted threshold there, which is consistent with the fact that the majority of the cores are not star forming. As our observations provide a lower limit of the

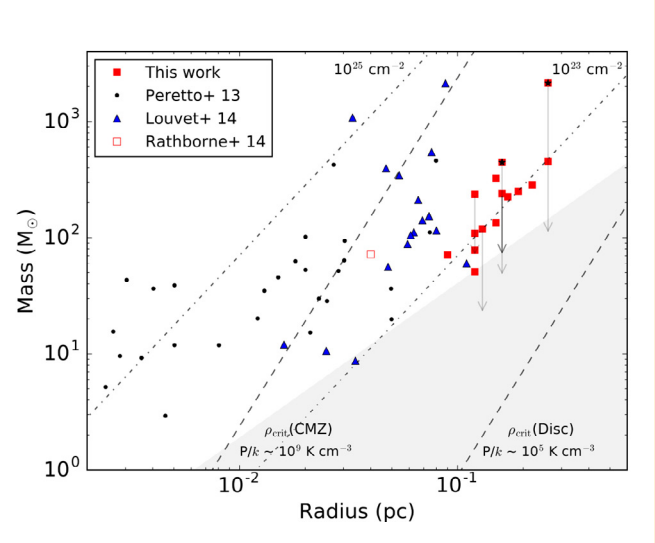

Figure 2: Mass-radius plot for all of the cores reported in our SMA sample. The solid red squares correspond to masses estimated assuming a dust temperature of 20 K and arrows indicate the possible range of mass, given strong lower-mass limits estimated, assuming (where possible) that the dust temperature is the same as the measured gas temperature. The red points with black star markers indicate that these cores are star forming. Black points correspond to high-mass protostellar cores in the Galactic disc taken from Peretto et al. (2013) and blue triangles to those from Louvet et al. (2014). The open red square corresponds to the star-forming core in cloud 'a' (aka 'the brick') as seen with ALMA observations (Rathborne et al. 2014). Dash/dot lines show constant column density. Dashed lines show the predicted critical volume density thresholds for both the CMZ and the Galactic disc, assuming pressures of P/k = 10^9 cm^{-3} and 10^5 K cm^{-3}, respectively. The grey shaded region corresponds to the empirical massive star formation threshold proposed by Kauffmann & Pillai (2010).

density on 0.1 pc scales, it is likely that the two protostars that we have discovered in the dust ridge are more compact than the resolution of our SMA observations, and are therefore likely at much higher local densities.

Further analysis of the full *CMZoom* catalogue (Battersby et al. in prep.; Hatchfield et al. in prep.), coupled with multiple on-going ALMA follow-up observations, promises to provide an unparalleled insight into the on-going and potential future star formation throughout this extreme environment, and ultimately advance our understanding of the environmental dependence of the star formation proces.

REFERENCES:

- Barnes A. T. et al., 2017, MNRAS, 469, 2263
- Battersby C. et al., 2017, IAU Symp. 322, 90
- Ginsburg A. et al., 2016a, A&A, 586, A50
- Ginsburg A. et al, 2018, ApJ, 853, 171
- Immer K. et al., 2012, A&A, 548, A120
- Immer K. et al., 2016, A&A, 595, A94
- Kauffmann J., Pillai T., 2010, ApJ, 723, L7
- Kruijssen J. M. D., Longmore S. N., 2013, MNRAS, 435, 2598
- Kruijssen J. M. D. et al., 2014, MNRAS, 440, 3370
- Krumholz M. R., McKee C. F., 2005, ApJ, 630, 250
- Longmore S. N. et al., 2013a, MNRAS, 429, 987
- Longmore S. N. et al., 2014, PPVI, 291
- Louvet F. et al., 2014, A&A, 570, A15
- Padoan P., Nordlund Å., 2011, ApJ, 730, 40
- Peretto N. et al., 2013, A&A, 555, A112
- Rathborne J. M. et al., 2014, ApJ, 795, L25
- Reid M. J. et al., 2014, ApJ, 783, 130
- Rosolowsky E. et al., 2010, ApJS, 188, 123
- Shetty R. et al., 2012, MNRAS, 425, 720
- Walker et al, 2018, MNRAS, 474, 2373

MOLECULAR RECONNAISSANCE OF THE β PICTORIS EXOCOMETARY GAS DISK

Luca Matrà, David J. Wilner, Karin I. Öberg, Sean M. Andrews, Ryan A. Loomis[1], Mark C. Wyatt[2], William R. F. Dent[3]

Sensitive searches are steadily adding to the number of planetesimal belts around nearby stars – analogues of our Kuiper belt – showing CO line emission, now comprising 15 systems (e.g. Moor et al. 2017). The wide range of ages for these belt-hosting systems advocates for this CO gas to be produced by release from icy exocomets. This exocomet scenario has been confirmed as the origin of the observed CO gas in four systems (Marino et al. 2016, 2017, Matrà et al. 2017a,b), where CO molecules are continuously released by cometary outgassing and then rapidly destroyed by UV radiation. This has allowed linking the observed CO gas mass to the exocometary CO content (Matrà et al. 2015), which already indicates a strong similarity between exocomets and Solar System comets (Matrà et al. 2017b).

The next step in investigating this compositional similarity between exocomets and Solar system comets requires information on other molecular species, to probe relative ice abundances. This information promises to shed light on the exocometary outgassing mechanism and on the chemical history of cometary volatiles across planetary systems. The most famous and best studied of these planetesimal belts is the one around the relatively young (23 Myr-old) A star β Pictoris, lying only 19.4 parsecs away from Earth. Early ALMA observations discovered copious amounts of CO gas within this belt, with a clumpy distribution indicating exocometary release at specific locations (Dent et al. 2014). We therefore set out to carry out a molecular survey of exocometary gas in the belt around β Pictoris with the SMA, covering lines of CO, CN, HCN, HCO^+, N_2H^+, H_2CO, H_2S, CH_3OH, SiO, and DCN (and complemented by archival ALMA observations).

We observed the β Pictoris belt with the SMA over two tracks in a compact antenna configuration at wavelengths near 1.1 and 1.3 mm. The southern location of β Pictoris (declination of -51°) makes it a challenging target for the SMA, since it is available only at high air mass (and rising above 15° elevation for only about 3 hours). Nonetheless, as **Figure 1** shows, SMA observations in good weather conditions provided a clear, resolved detection of continuum emission and CO J=2-1 line emission from the belt, with spatial distribution (including the asymmetry discovered by ALMA) and flux levels consistent with previous measurements. As **Figure 2** shows, however, the SMA data cubes show no significant detections around the spectral locations corresponding to the CN N = 2-1, HCN J = 3-2, HCO^+ J = 3-2 , N_2H^+ J = 3-2, and H_2CO J = $4_{1,4}$-$3_{1,3}$ lines. Similarly, no significant emission was observed in the archival ALMA data cubes around the H_2S $2_{2,0}$-$2_{1,1}$ CH_3OH $5_{1,4}$-$4_{2,2}$, SiO J = 5-4, and DCN J = 3-2 lines.

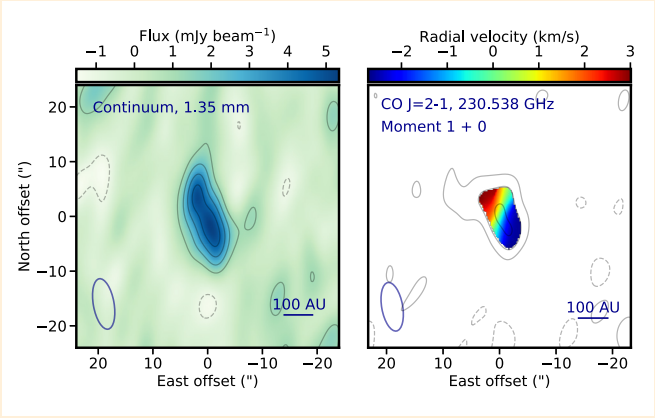

Figure 1: Left: SMA 1.35 mm continuum image of the β Pictoris disk. **Right:** Contours show the moment 0 (spectrally integrated) map of the CO J = 2-1 line. The color scale (moment 1 map) represents the velocity field of the disk, i.e., the centroid velocity of the line (with respect to the star) at each spatial location. In both panels, the ellipse in the bottom left represents the synthesized beam, and contours are drawn at intervals of two times the RMS noise level.

We set out to connect these line flux upper limits to exocomet ice compositions relative to CO using the steady-state exocome-

[1]CfA; [2]Institute of Astronomy, University of Cambridge, UK; [3]ALMA SCO, Santiago, Chile

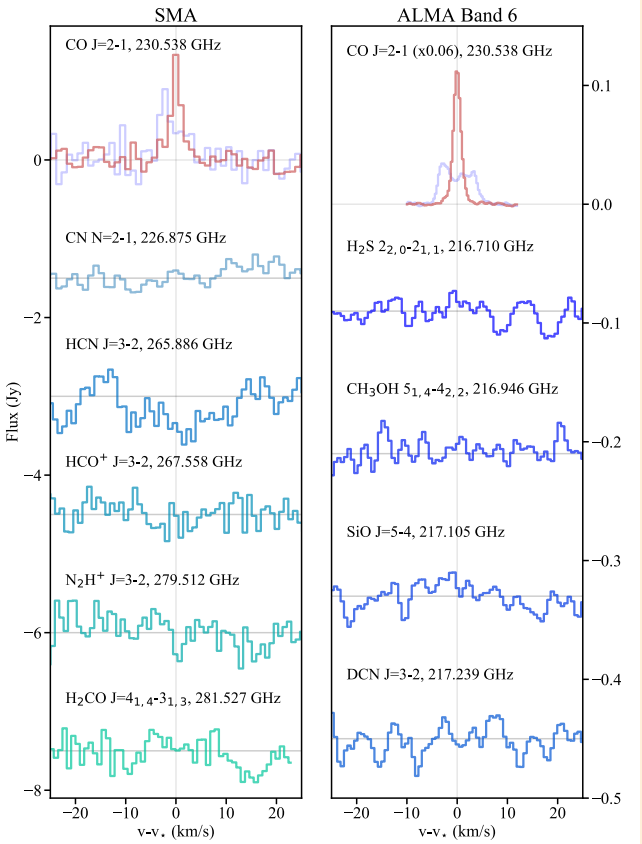

Figure 2: Spectra of the lines targeted in our SMA survey (left) and in archival ALMA data (right). For the CO J = 2-1 line (top row), we show the effect of our spectrospatial filtering technique. This has also been applied to boost the SNR and increase the chance of detection for the other molecular lines shown here, which however remain undetected.

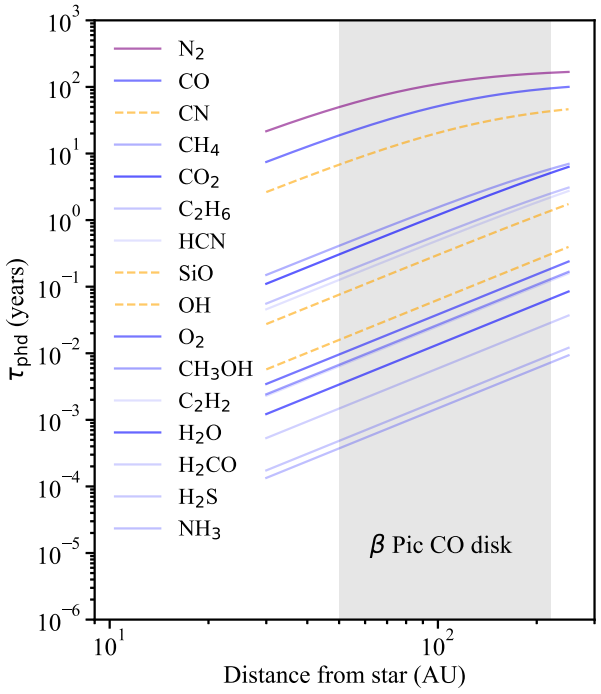

Figure 3: Unshielded photodissociation timescales of molecular gas species observed in solar system comets. Species are listed in order of their timescale, from longest lived to shortest lived, and are therefore in the same vertical order as the corresponding lines (though note that the C_2H_2 line overlaps the CH_3OH line). The transparency of the blue solid lines is set to indicate their log-scale abundance in solar system cometary ice with respect to H_2O, darker for more abundant species. The purple line is for N_2, by far the least abundant of all listed species from measurements in comet 67P (Rubin et al. 2015). Orange dashed lines represent daughter species (CN, OH) or species that we observed but are not detected in solar system comets (SiO).

tary gas release model developed by Matrà et al. 2015 and 2017b. Connecting these data to outgassing rates for different species requires calculating their non-local thermodynamic equilibrium (NLTE) excitation and their photodissociation timescale against stellar and interstellar UV radiation, which determines how long a molecule will survive once released from the exocometary ice. **Figure 3** shows the photodissociation timescale in years for a range of commonly observed Solar System cometary molecules around a star like β Pictoris. The harsh UV radiation field causes photodestruction of the vast majority of volatile species on very short timescales of days to months; therefore, photodissociation alone can explain most of the upper limits. The longest lasting molecules by far are N_2, CO, and CN, having unshielded photodissociation timescales of 96, 42, and 16 years, at least an order of magnitude longer than for any other molecular species. Given that N_2 lacks a strong dipole moment necessary for detection, the only observable molecule with a survival timescale similar to that of the detected CO is CN, which we focus on here. In Solar System comets, CN gas is produced mainly by photodissociation of HCN gas (Fray et al. 2005); we assume the same applies for exocomets around β Pictoris, and that CN is a direct tracer of HCN. We then built a NLTE excitation model for the CN and CO molecules including fluorescence caused by absorption of stellar UV light and subsequent decay to the lower (rotational) energy levels that we observed. This is crucial for accurate determination of CN (and CO) masses in low density, optically thin environments typical of exocometary gas in planetesimal belts. Combining gas masses to photodissociation timescales for both molecules, under the steady state assumption, allows an estimate of the ratio of exocometary outgassing rates of HCN (as traced by CN) compared to CO, which is a measure of the rate at which HCN is being released from the ice with respect to CO. Since we have only an upper limit on the CN mass, for now we can only set an upper limit on the HCN/CO outgassing rate ratio.

Figure 4 compares this upper limit to known HCN/(CO+CO_2) outgassing ratios from Solar System comets, where we include CO_2 as a likely contributor to the observed CO emission (due to the rapid photodissociation of CO_2 into CO). We find that our upper limit of 2.5% on the HCN/(CO+CO_2) outgassing rate ratio in

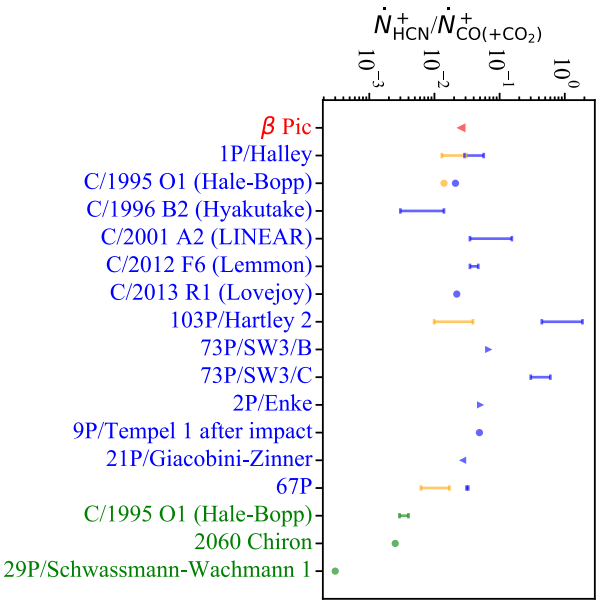

Figure 4: Spectra of the lines targeted in our SMA survey (left) and in archival Comparison between our measured upper limit on the HCN/($CO+CO_2$) ratio of outgassing rates in β Pictoris (red) with solar system comets. For solar system comets, symbols represent the HCN/($CO+CO_2$) outgassing ratios (orange, where available) or HCN/CO outgassing ratios (blue) reported by Le Roy et al. (2015) and references therein. We use solid circles where a single value is reported and vertical bars where a range of values is reported. Upward and downward pointing triangles represent lower and upper limits, respectively. Green points are HCN/CO measurements for comets observed at large distances from the Sun (Hale-Bopp at 4.6-6.8 au, Chiron at 8.5-11 au, and 29P at 5.8 au, Womack et al. 2017), where different thermal outgassing rates are expected for CO and HCN.

β Pic's exocometary gas is consistent with, although below most of, the values measured in Solar System comets as observed near Earth. If deeper observations push this limit down to prove a significant depletion compared to Solar System comets, then this could mean either that there is a true depletion of HCN compared to CO and CO_2 in exocometary ices around β Pic, or that the outgassing mechanism is such that β Pic's exocomets release CO but not HCN.

In general, we find that outgassing ratios of observed molecular species should reflect their ice compositions as long as ices cannot survive on grains down to the smallest sizes and be removed from the system through radiation pressure from the central star. This is likely true for β Pic's exocomets, as (1) collisions between them will allow ice layers to resurface, where they become subject to rapid UV photodesorption (Grigorieva et al. 2007), and (2) the smallest unbound grains will undergo hypervelocity collisions on their way out of the system, leading to vaporization of any ice that may have survived on these grains (Czechowski & Mann 2007). These processes will allow release of molecules less volatile than CO, such as HCN, that would otherwise survive in the ice phase on the smallest grains and be removed dynamically by radiation pressure from the central star. If so, then a low HCN/($CO+CO_2$) outgassing rate would indicate a low HCN/($CO+CO_2$) abundance in the exocometary ice.

The abundance of HCN in exocomets is especially interesting because of its connections to origins of life chemistry (e.g., Powner et al. 2009). The large scatter in HCN abundances observed among solar system comets (Mumma & Charnley 2011, and references therein) and observations of cyanides in protoplanetary disks (e.g. Öberg et al. 2015) indicate that cometary cyanides may not be directly inherited from the ISM, but instead arise from active chemical processing during the epoch of planet formation. Whether the endpoint of this chemistry is different for different planetary systems is as yet unclear and can be resolved only by future, deeper observations of exocometary cyanides.

REFERENCES:

- Czechowski, A., & Mann, I. 2007, ApJ, 660, 1541
- Dent, W. R. F., Wyatt, M. C., Roberge, A., et al. 2014, Sci, 343, 1490
- Fray, N., Bénilan, Y., Cottin, H., Gazeau, M.-C., & Crovisier, J. 2005, P&SS, 53, 1243
- Grigorieva, A., Thébault, P., Artymowicz, P., & Brandeker, A. 2007, A&A, 475, 755
- Le Roy, L., Altwegg, K., Balsiger, H., et al. 2015, A&A, 583, A1
- Marino, S., Matrà L., Stark, C., et al. 2016, MNRAS, 460, 2933
- Marino, S., Wyatt, M. C., Panić, O., et al. 2017, MNRAS, 465, 2595
- Matrà L., Dent, W. R. F., Wyatt, M. C., et al. 2017a, MNRAS, 464, 1415
- Matrà L., MacGregor, M. A., Kalas, P., et al. 2017b, ApJ, 842, 9
- Matrà L., Panić, O., Wyatt, M. C., & Dent, W. R. F. 2015, MNRAS, 447, 3936
- Moór, A., Curé, M., Kóspál, Á, et al. 2017, ApJ, 849, 123
- Mumma, M. J., & Charnley, S. B. 2011, ARA&A, 49, 471
- Öberg, K. I., Guzmán, V. V., Furuya, K., et al. 2015, Natur, 520, 198
- Powner, M. W., Gerland, B., & Sutherland, J. D. 2009, Natur, 459, 239
- Rubin, M., Altwegg, K., Balsiger, H., et al. 2015, Sci, 348, 232
- Womack, M., Sarid, G., & Wierzchos, K. 2017, PASP, 129, 031001

RESOLVED MILLIMETER OBSERVATIONS OF THE HR 8799 DEBRIS DISK

David J. Wilner[1], Meredith A. MacGregor[2], Sean M. Andrews[1], A. Meredith Hughes[3], Brenda Matthews[4], Kate Su[5]

The young (30 Myr) and nearby (40.4 pc) A-type star HR 8799 is the host of the first (and so far only) directly imaged multiple planet system. Near-infrared images show four companions with projected separations of 14, 24, 38, and 68 AU (Marois et al. 2008, 2010), and their orbital motions have been tracked for more than a decade (e.g. Bowler 2016). Comparison of infrared photometry with standard evolutionary models suggests these companions have masses in the range of 5 to 10 Jupiter masses (Marley et al. 2012), consistent with various dynamical calculations that imply masses less than 10 Jupiter masses for stability at the system age. In addition to these planetary mass companions, HR 8799 also hosts a debris disk first detected by IRAS. Multi-wavelength studies show that the debris consists of a warm (T~150 K) inner belt and a cold (T~35 K) outer belt that bracket the orbits of the directly imaged planets, plus a halo of small grains that extend to radii beyond 1000 AU (Su et al. 2009). Since millimeter emission selectively reveals the large dust grains less affected by radiative forces that trace best the parent planetesimals, we used the SMA to obtain new observations at 1.3 mm that improve on previous attempts. Wilner et al. (2018) provide a full description of this work.

Submillimeter photometry marks the HR 8799 debris disk as one of the most massive known, at about 0.1 Earth masses (Williams and Andrews 2006), but detailed millimeter imaging has proved to be challenging. Single dish observations from the CSO at 350 microns (9 arcsec beam) resolved emission from the cold belt around the star, with a tentative offset asymmetry (Patience et al. 2011) that was not confirmed by observations with the JCMT at 450 and 850 microns (8 and 13 arcsec beam, respectively) (Holland et al. 2017). Hughes et al. (2011) made the first millimeter interferometric detection of the disk, using the SMA at 870 microns, consistent with the presence of a broad belt but insufficient to derive accurate structural parameters. More recently, Booth et al. (2016) presented ALMA observations at 1.3 mm with much higher sensitivity, but these observations recovered only a small fraction of the total disk emission. By making new SMA observations in the subcompact configuration at 1.3 mm, we obtained sensitivity to larger angular scales than the previous millimeter

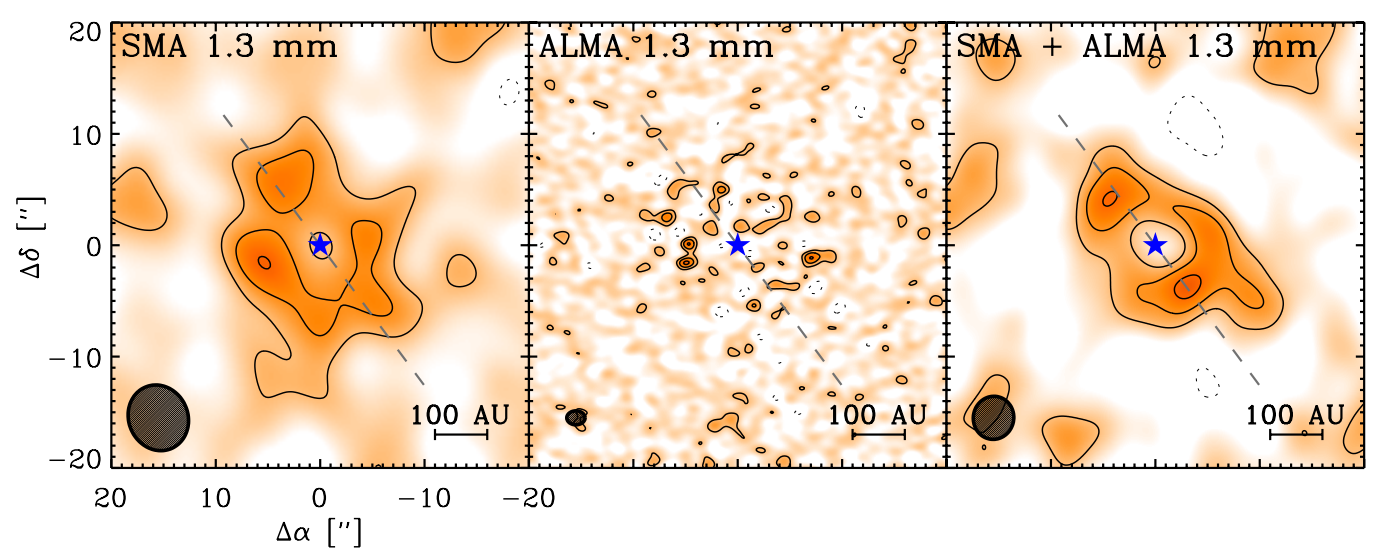

Figure 1: Images of 1.3 mm continuum emission from the HR 8799 debris disk from the SMA (left), ALMA (center), and the SMA and ALMA combined (right), from Wilner et al. (2018). All of these images were made with natural weighting, and those including SMA data use a 4 arcsec FWHM Gaussian taper. Contour levels are in steps of 2x the measured rms values of 180 microJy/beam, 16 microJy/beam, and 30 microJy/beam for the three images, respectively. The beam sizes are shown by the ellipses in the lower left corner of each image and are 6.1x5.6 arcsec, 1.7x1.2 arcsec, and 3.8x3.7 arcsec. The blue star symbol indicates the stellar position, and the dashed gray line shows the orientation of the best-fit model emission belt.

[1]CfA; [2]Carnegie DTM; [3]Wesleyan; [4]NRC Herzberg; [5]U. Arizona

interferometer studies and recovered essentially all of the disk emission. By modeling these new SMA data, together with the archival ALMA data, we obtained a much better characterization of the underlying planetesimal distribution. We also obtained photometry of the disk with the VLA at 9 mm in the most compact D configuration. With this information, we examined (1) the belt geometry constraints in the context of coplanarity and alignment of the planetary system, (2) the relationship between the belt inner edge and the outermost planet b, (3) ramifications of the radial surface density profile for collisional excitation mechanisms, (4) molecular line emission from the region, and (5) the millimeter spectral index connections to collisional models.

Figure 1 shows the 1.3 mm continuum images of HR 8799 from the SMA (left), ALMA (middle), and the combination of SMA and ALMA (right). These images were obtained with natural weighting, and those including SMA data use a 4 arcsec FWHM Gaussian taper to improve surface brightness sensitivity at the expense of angular resolution. The ALMA image is comparable to Figure 1 of Booth et al 2016, with a beam size of about 1.5 arcsec, and it shows a noisy ring of emission surrounding the star. For the SMA image, the beam size is 4 times larger in each dimension than for the ALMA image, and the noise level is an order of magnitude higher, but the sensitivity to larger angular scales provided by the shorter baselines enables a much improved representation of the radially extended belt of emission around the star. The combination of SMA and ALMA data results in an even better image of this circumstellar structure. The two peaks visible on either side of the star are the signatures of limb brightening along the major axis of an inclined, optically thin emission belt. These data provide no evidence for significant clumps or other asymmetries that might result from sculpting of the belt by the gravity of planets.

To provide a quantitative characterization of the 1.3 mm emission from the disk, we make the simple assumption that the structure can be represented by an axisymmetric and geometrically thin belt, and we model the observations using the visibility fitting procedure described by MacGregor et al. 2013. We fit the belt surface brightness by a radial power law with power law index x, between an inner and outer radius, R_{in} and R_{out}, in an MCMC framework. We note that modeling the ALMA observations did not produce informative constraints for the belt outer radius (or total flux), most likely because the ALMA primary beam is comparable in size to the emission region, and the ALMA observations provide very little data at spatial frequencies inside the first null of the visibility function to limit the emission. By contrast, modeling the SMA and ALMA observations together provided strong constraints on the important belt parameters: total flux 3.44 (+0.31,-0.56) mJy, inner edge 104.0 (+8.0,-12.0) AU, outer edge 361.0 (+16.0,-18.0) AU, power-law index -0.38 (+0.47,-0.47), inclination 32.8 (+5.6,-9.6) degrees, position angle 35.6 (+9.4,-10.1) degrees.

The millimeter belt inclination and position angle overlap with estimates of the orbital inclination and angle of ascending node of the planet orbits determined by astrometric monitoring. These are consistent with a coplanar configuration of the disk and planetary orbits, although the mutual uncertainties are still large and preclude firm conclusions on this point. There is some tension between these millimeter fits and the debris disk geometry determined from the shape of the far-infrared emission in Herschel images, which indicate an inclination of 26 (+3,-3) degrees and position angle 64 (+3,-3) degrees, although these differences may have a physical origin in size-dependent dust dynamics.

The best-fit inner edge of the millimeter emission belt provides an independent constraint on the mass of the outermost planet b, under the assumption that the chaotic zone of this planet truncates the planetesimal disk. This is important because the planet evolutionary models are highly degenerate in planet mass, luminosity and age, in part because the effects of initial conditions, e.g. initial thermal content, can persist for 100's of Myr. In principle, independent constraints on planet mass from dynamics can break these degeneracies. Such constraints have the potential to help distinguish planet formation models, in particular hot-start models where most entropy is retained, e.g. by gas that collapses directly to form planets, from cold-start models where most entropy is lost, e.g. by gas cooling in core accretion. Notably, the core accretion model is challenged to form 5 to 10 Jupiter mass planets at the large orbital radii of the HR 8799 planets. Using the expression obtained by Pierce and Wyatt (2014), we translate the inner edge constraint directly into a planet b mass constraint of 5.8 (+7.9,-3.1) Jupiter masses. Although the uncertainties are still large enough to allow for a range of initial thermal content, it is encouraging that the mass is compatible with estimates obtained from the planet b luminosity and standard evolutionary models. Given this result, there is no need to posit the presence of an additional unseen planet beyond planet b, or variations in the orbit of planet b, to account for the disk truncation (Booth et al. 2016).

The planetesimals within the debris disk must be stirred to incite destructive collisions to produce the observable dust. The two leading mechanisms for this stirring process are "self-stirring" by an outwardly moving front of planetoid formation and growth (Kenyon and Bromley 2002) and "planet-stirring" by the gravitational influence of interior giant planets. Moor et al. (2015) suggested that the HR 8799 debris disk is planet-stirred, given the young age of the system and the large extent of the debris disk. An additional observable that can help discriminate stirring scenarios is the radial distribution of the planetesimals, since self-stirred models produce an extended planetesimal disk with an outwardly increasing surface density (Kennedy and Wyatt 2010) while standard steady-state debris disk models tend to produce surface density profiles that do not increase with radius (e.g. Krivov et al. 2006). If we assume that the radial temperature profile is determined by radiative equilibrium with stellar heating, then the best-fit radial power-law index for the emission suggests a flat or shallow surface density profile. This result disfavors self-stirring. For this system, it seems plausible that the giant planets responsible for stirring the debris disk are detected directly.

With SWARM, the SMA observations included the ^{12}CO and ^{13}CO J=2-1 lines with channel spacing 140 kHz, corresponding to about 0.18 km/s. Emission from these lines was detected over the narrow LSR velocity range -6 to -4 km/s, close to the stellar velocity (-4.6 km/s in this frame). Previous JCMT observations

of the ^{12}CO J=3-2 line show extended emission concentrated in a filament, likely associated with the MBM 53-55 complex of high latitude clouds (Williams and Andrews 2006, Su et al. 2009). Unfortunately, as in previous attempts to use interferometers to image the molecular line emission in this region, the extended emission remains poorly sampled and problematic to reconstruct, even with the lower spatial frequency data newly obtained with the SMA. All attempts at imaging show strong artifacts due to missing flux, and there is no clear evidence for any systematic motions that might be associated with rotation of gas in the debris disk.

Flux density measurements from the SMA at 1.3 mm, 3.44 (+0.31,-0.56) mJy, and the VLA at 9mm, 32.6 (+9.9,-9.9) microJy, give a spectral index of 2.41 (+0.17,-0.17). For standard assumptions about grain properties, this implies a grain size distribution with power index q = 3.27 (+0.10,-0.10), a value consistent with the mean value of the spectral indices found for a sample of more than a dozen other debris disks over a similar wavelength range (MacGregor et al. 2016). This power law size distribution is close to the prediction for the classical scale-free steady-state collisional cascade, with no need to invoke any additional complexities in the collisional model, such as size dependent velocities or material strengths.

In summary, new SMA observations have improved our view of the large-scale spatial distribution of the planetesimals within the debris disk that surrounds the HR 8799 planetary system. However, these observations still do not have sufficient sensitivity to reveal any details of planet-disk interactions, or to obtain dynamical constraints on the planet b mass that usefully discriminate evolutionary models. Since the planet mass constraints scales steeply with the disk-planet separation, a more accurate determination of the of the inner edge of the millimeter emission belt could significantly improve the planet b mass constraint. A better constraint obtained in this way, e.g. with deeper SMA observations, or ALMA ACA observations, could provide important feedback into the system dynamics, planet cooling models, and planet formation scenarios, and also show if a more sophisticated approach is needed for modeling and interpretation.

REFERENCES:

- Booth, M., Jordan, A., Casassus, S., et al. 2016, MNRAS, 460, L10
- Bowler, B.P. 2016, PASP, 128, 102001
- Holland, W.S., Matthews, B.C., Kennedy, G.M., et al. 2017, MNRAS, 470, 3606
- Hughes, A.M., Wilner, D.J., Andrews, S.M., et al. 2011, ApJ, 740, 38
- Kenyon, S.J., & Bromley, B.C. 2002, ApJ, 577, L35
- Kennedy, G.M., & Wyatt, M.C. 2010, MNRAS, 405, 1253
- Krivov, A.V., Lohne, T., & Sremvcevic, M. 2006, A&A, 455, 509
- MacGregor, M.A., Wilner, D.J., Andrews, S.M., et al. 2015, ApJ, 809, 47
- Marley, M.S., Saumon, D., Cushing, M., et al. 2012, ApJ, 754, 135
- Marois, C., Macintosh, B., Barman, T., et al. 2008, Science, 322, 1348
- Marois, C., Zuckerman, B., Konopacky, Q.M., et al. 2010, Nature, 468, 108
- Moor, A., Kospal, A., Abraham, P., et al. 2015, MNRAS, 447, 577
- Patience, J., Bulger, J., King, R.R., et al. 2011, A&A, 531, L17
- Pearce, T.D., & Wyatt, M.C. 2014, MNRAS, 443, 2541
- Su, K.Y.L., Rieke, G.H., Stapelfeldt, K.R., et al. 2009, ApJ, 705, 314
- Williams, J.P., & Andrews, S.M. 2006, ApJ, 653, 1480
- Wilner, D.J., MacGregor, M.A., Andrews, S.M., et al. 2018, ApJ, 855, 56

THE SUBMILLIMETER ARRAY NEEDS SOME RASPBERRY PIs!!

Ramprasad Rao (ASIAA), Paul Grimes (SAO), Steve Leiker (SAO), and the SMA technical team.

In the past few years, the advent of the small Raspberry Pi computer has triggered a mini-revolution in the embedded computing arena. For under $40, one can get this ARM processor equipped computer running a modern Linux operating system with a footprint about the size of half of a standard paperback novel. The newest version, the Raspberry Pi 3 Model B+, comes with a plethora of ports including 4 USB 2.0 ports, a Gigabit ethernet port, built-in wireless technologies including wi-fi and bluetooth*, a camera port, and audio out, along with an HDMI port to connect to an external display. But it is not this abundance of ports that gives this little board its mighty powers. The magic comes from 40-pins neatly arranged in two rows of twenty pins each, that almost span the entire length on one side of this board. This 40-pin connector goes by the fancy name of General Purpose Input/Output or GPIO in short. This set of pins can control devices ranging from a simple LED to assorted motors, and interface with fancy

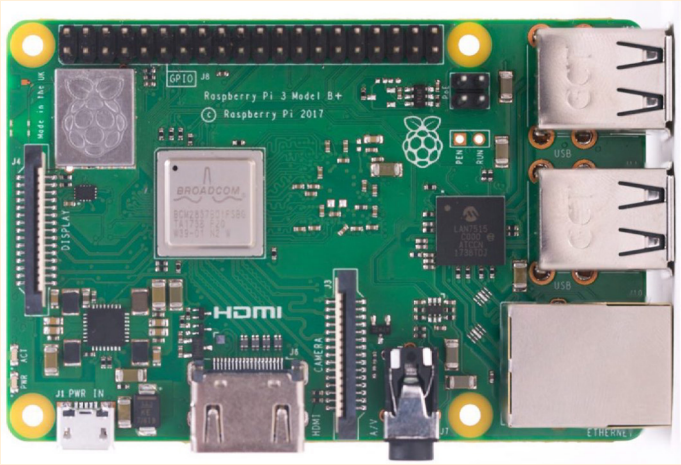

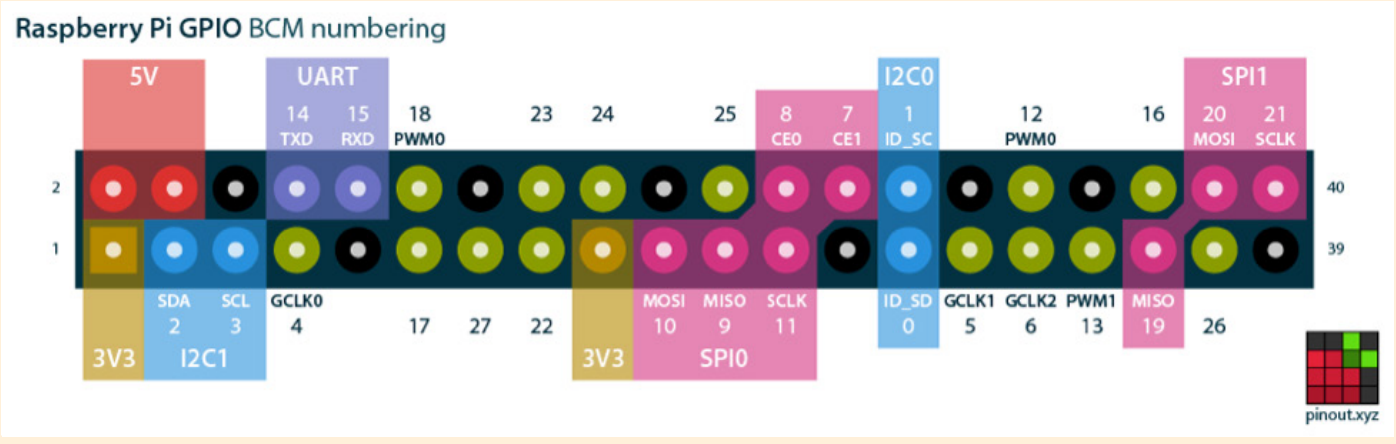

Figure 1. The top image shows the most recent version of the Raspberry Pi single board computer, version 3 model B+. The CPU used is the BCM2837B0, Cortex-A53 (ARMv8) 64-bit SoC @ 1.4GHz. The bottom image shows the pin layout and numbering scheme. For more information, see https://www.raspberrypi.org/products/raspberry-pi-3-model-b-plus/ and https://pinout.xyz/pinout/.

*We will ensure that this is disabled at the summit to minimize radio interference :)

custom designed boards. This set of 40 GPIO pin along with the Raspberry PI OS, has support for protocols with a veritable alphabet soup of names such as I2C, UART, SPI, PCM, and PWM in addition to standard garden variety GPIO (See **Figure 1**). This flexibility and access to digital ports has led to the emergence of a wide and largely "open" hardware and software ecosystem, using Pis for everything from home automation to CubeSat space missions. Using the technologies present within the Raspberry Pi ecosystem, a number of useful applications have already been prototyped and developed at the Submillimeter Array. One application in development, the scanning spectrometer, which uses a Raspberry Pi for control and monitoring, was showcased in the previous newsletter (Jan 2018). In this article, we will mention other ongoing examples and future applications in development which rely on a Raspberry Pi.

One such simple application is the use of a Raspberry Pi camera along with an LED light to monitor the orientation of the quarter waveplate. This monitoring was needed as the orientation of the waveplate on one of the antenna assemblies had changed, likely during shipping or transport. An error in orientation by just one degree can introduce an unwanted instrumental polarization of almost 2% and thus it is necessary to rectify this. Taking advantage of its compact size, the Raspberry Pi camera, the computer, and the LED were mounted to the calibration load assembly to look at the angular markings on the rotational positioning assembly. Measuring the signal modulation while rotating the waveplate through a range of small angles allows us to determine the optimal position with lowest instrumental polarization to a fraction of a degree. To illustrate the simplicity, the following three commands are all it takes to make this application work.

```
gpio write 7 1
```
(turns on the LED connected to GPIO pin 7;
it is dark in the antenna with lights off)

```
raspistill -o image.png
```
(takes the picture)

```
gpio write 7 0
```
(turns off the LED)

Another recent application of the Raspberry Pi is the development of a reference optics insert to ensure correct alignment of the grid and the combiner mirror which are part of the SMA optics cage. This reference insert integrates a compact touch-capable LCD display along with dual Raspberry Pi cameras with an off-the-shelf multi-camera adapter module, and draws power from a run of the mill power bank (See **Figure 2**). This is a completely stand-alone unit and can be easily switched from one optics insert position to another in a few minutes. One camera is pointed at the wire grid while the second is pointed at the combiner mirror. Comparing the pictures to a fiducial reference picture which was accurately aligned in the laboratory allows us to determine the optimum position of the grid or mirror. Camera selection is made by signaling various GPIO pins to ground or high. This can be done using commands similar to those shown in the previous example. However, this application functioned by embedding both the GPIO commands and picture capture commands within a Python program. An external Python module for GPIO control is provided by the Raspberry Pi operating system. One of the advantages of the Raspberry Pi ecosystem is those vast repositories of Python based drivers for device control and application software which are available for a wide variety of applications. We plan to take full advantage of this freely available resource which will save time spent on developing custom software.

Figure 2. The above figure shows the reference optics insert with the integrated Raspberry Pi and dual camera setup. Since this is powered with a USB power bank, it can be used as a stand-alone unit. This unit was developed by Lingzhen Zeng.

While the above two applications have been more at the level of prototypes, the next step is to design and develop a Raspberry Pi based distributed system for monitoring and controlling the next generation wideband SMA receivers, replacing the array of custom programmed microcontrollers in use on the current receiver system. This is a much more complex and mission critical system

Figure 3. The above figure shows the most recent version of the Raspberry Pi Patch. This features 7 Pis with separate external ethernet ports which can be used also as Power Over Ethernet (POE). (Photo credit: Steve Leiker).

that will have the ability to perform such operations such as setting and reading voltages, currents, and magnetic field currents on the SIS mixer. This should also be able to control various local oscillator settings such as voltages and power levels among other things. These operations require the design and development of add-on boards (daughter/grand-daughter boards) that will be attached to the 40-pin GPIO connector to communicate with the Pi and thus the wider SMA control system. Each of the daughter boards has i) two Analog-to-Digital converters (ADC) which can read a total of eight single-ended analog inputs or four differential inputs, ii) two Digital-to-Analog converters (DAC) which can output a total of eight analog voltages, and iii) two Digital-Input-Output (DIO) modules which can either input or output a total of sixteen digital signals. These daughter boards have been prototyped and some early units have been assembled and tested in Hilo. We are anticipating that we will need about six to eight Raspberry Pis to control all of the electronics and receiver systems in each antenna.

There will be a total of 75 or more Raspberry Pi computers in the SMA network and this poses a challenge to maintain and deploy. As the Raspberry Pis will be crucial to the operation of the wSMA Receiver System, we are making tests to demonstrate that Pis can operate reliably in the SMA telescope environment.Three sets of Pi-Patch rack mountable units have been constructed – one for testing in Hilo, and two that have been deployed at the summit in Antenna 3 and Antenna 7. Each Pi-Patch unit contains multiple Raspberry Pi computers (See **Figure 3**). The last of the units also had the ability to use Power-over-Ethernet which would enable remote power cycling if needed. The units at the summit have been operational for more than 8 months without any failures while running at full cpu load.

One particular concern is that the Raspberry Pi computer, which uses a micro-SD card for the root file system, may exhibit failure after a large number of read-write cycles, particularly if power cycling occurs during the process of writing to the SD card. In order to avoid this potential failure, we are working on a solution that will net-boot the Raspberry Pi's using a central 'tftpboot' server. This centralized server will provide a common root-filesystem for each of the computers and eliminate the need for a micro-SD card to boot or operate the Pi. The primary applications which will run on these Raspberry Pis for monitoring and control, as well as other configuration files, will reside on a different server which will export the directories using an 'nfs' file system. This system of distributed computers with remote filesystem hosting is designed to simplify operational use, maintenance, and deployment. This netbooting methodology is currently being stress tested in Hilo on a system containing seven Raspberry Pi's for reliability and has been functioning since April. In early summer of 2018, this netbooted system will be deployed to the summit into one of the antennas for additional summit network tests.

THE 2018 EVENT HORIZON TELESCOPE OBSERVING CAMPAIGN

64 GBPS DOUBLE SIDEBAND PHASED ARRAY VLBI AT SUBMILLIMETER ARRAY

Jonathan Weintroub & André Young

The Submillimeter Array (SMA) participated in the April 2018 Event Horizon Telescope (EHT) observing campaign with SWARM running at the full targeted EHT bandwidth, implementing a *double sideband* phased array for the very first time. With a recording data rate of 64 gigabits-per-second (Gbps) the SMA station alone produced about a petabyte of recorded phased array data over the six EHT observing tracks. Not only this, but the SMA, SWARM and the SWARM VLBI Digital Back Ends (SDBE) operated without a technical hitch over the campaign—apart from a slight weather delay on the first night—with the full data rate uniformly recorded.

Overall, the EHT observed with a larger array than ever before for six full coordinated tracks in April 2018. The array consisted of nine participating telescopes at seven geographic locations. The SAO-ASIAA collaboratively developed and operated Greenland Telescope (GLT, Thule, Greenland) participated in EHT observations for the first time. The other eight facilities were the South Pole Telescope (SPT), Atacama Pathfinder Experiment (APEX), Atacama Large mm/Submm Array (ALMA), Large Millimeter Telescope (LMT, Mexico), James Clerk Maxwell Telescope (JCMT, Maunakea), Arizona Radio Observatory Submillimeter Telescope (ARO-SMT, Mount Graham, Arizona) and the Institut de Radioastronomie Millimétrique Thirty Meter Telescope on (IRAM 30m, Pico Veleta, Spain), in addition to the Submillimeter Array.

The primary EHT targets were M87 and SgrA* as usual, though a broader set of AGN science targets including 1055+018, OJ287, and Cen A were observed. Markarian 501 was approved via the ALMA proposal process, conditional on a minimum flux density criterion, which it unfortunately did not meet. The observation nights were 20, 21, 23, 24, 26, 27 April. Sadly, the weather across the array was not as favorable as in 2017. At the SMA there was a break in the bad weather pattern of 2018 as the campaign began, which lasted about a week to benefit the EHT.

DOUBLE SIDEBAND SWARM PHASED ARRAY OPERATION

The 2018 EHT array-wide goal was to increase its observational bandwidth to 8 GHz per polarization or 16 GHz total, equivalent to a total recording data rate of 64 Gb/s. This represents a doubling of the bandwidth processed in 2017. The 8 GHz per polarization requires recording both upper and lower sidebands of the receiver at participating sites. The technical enhancements at the SMA to achieve this are fairly complex and represent a significant upgrade to SWARM.

Figure 1. Paul Yamaguchi, with very high tech de-icing equipment, readies the SMA for operations on night 1. The low cloud and fog you can see in the photo background lifted fairly abruptly after sunset. The SMA remained closed due to precipitation until just as the first EHT track started, but opened shortly thereafter. A few scans were off source as the SMA got set up (fringe confirmation, delay calibration, pointing). Thereafter SMA EHT operations were flawless.

Since SMA uses double sideband receivers, both upper and lower sideband signals are superimposed in the digitized intermediate frequency signal. By applying mutually orthogonal phase modulation patterns ("Walsh functions") to the local oscillator in the receiver of each antenna, the sidebands can be separated by applying the corresponding demodulation patterns to the digital data. Although this demodulation was already fully implemented for the connected element correlator of the SMA, only the demodulation for one sideband was implemented in the beam-

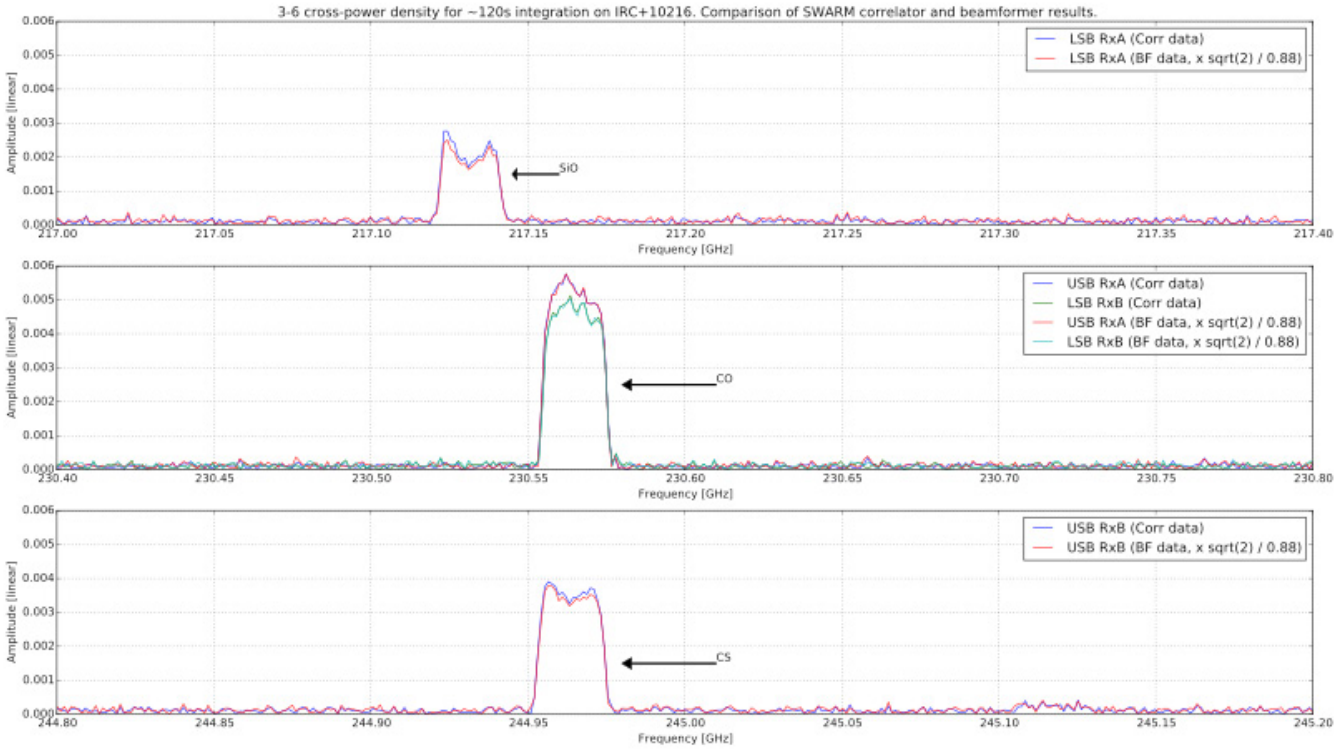

Figure 2. Test observations of three molecular lines in IRC+10216 positioned strategically in the lower and upper sidebands of two SMA receivers. During these tests the dual-receivers of the SMA were tuned such that the CO (J = 2 → 1) line appeared near the center of the processed bands for the upper sideband of one receiver and the lower sideband of the other receiver. In reading the above graphic. note that the top and bottom panels each show two measurements of a line, SiO in LSB, and CS in USB, respectively. The two measurements in each case are (i) from the SWARM real time cross-correlator and (ii) from non-real-time correlation for recorded phased array data. The middle panel has four measurements of the CO line, each pair produced in the same way as for top and bottom panels, with two pairs resulting because the tuning was arranged such that CO appears in the LSB of one of the receivers and the USB of the other in the same position in the spectrum. There is a somewhat large difference between the LSB and USB measurement, which we attribute to factors such as system temperature, pointing, and polarization differences across receivers not being controlled. Subject to certain correction scale factors, for example to account for 2-bit vs 4-bit efficiency, excellent agreement between correlator and beamformer results are obtained. Spectral lines are visible at comparable amplitudes in the lower and the upper sidebands, and appear the same whether calculated real-time by the SWARM cross-correlator, or using VLBI correlation from recorded data. We conclude that sideband separation is being accomplished properly in the recorded phased array data.

former which outputs the data used by the EHT. Allowing fully double sideband EHT observations at the SMA therefore required also implementing the second sideband Walsh demodulation in the beamformer.

In the time since the end of the 2017 April campaign SWARM has been upgraded to support second sideband recovery in the beamformer without adding further strain to the network infrastructure that connects the system's ROACH2 processors. In addition to applying the necessary sideband separating demodulation patterns, independent phasing weights are also required for the second sideband since the atmospheric phase, compensated for by the adaptive beamforming algorithm, has opposite sign in the two sidebands. A dedicated Ethernet output of that phased sideband is provided, and a Mark6 digital recorder is needed to record each sideband. The design was tested and verified at the SMA observing IRC+10216, which features many strong spectral lines. The tests took place over the course of several nights prior to April 2018, and the results are shown in figure 2 with a detailed explanatory caption.

APHIDS: INTERPOLATION AND DOWNSAMPLING

Single dish telescopes that employ the EHT-wide standard digital backend process the full frequency bandwidth in blocks that are each 2048 MHz wide, sampling each block at the Nyquist rate of 4096 MSa/s. The SMA processes its full bandwidth in blocks that are 2288 MHz wide, sampled at 4576 MSa/s each. In order to deliver to the EHT correlator an SMA data product that is fully compatible with the rest of the EHT, the SMA data need to be resampled at a lower rate. Furthermore, the raw beamformer data product recorded at the SMA is a frequency-domain sam-

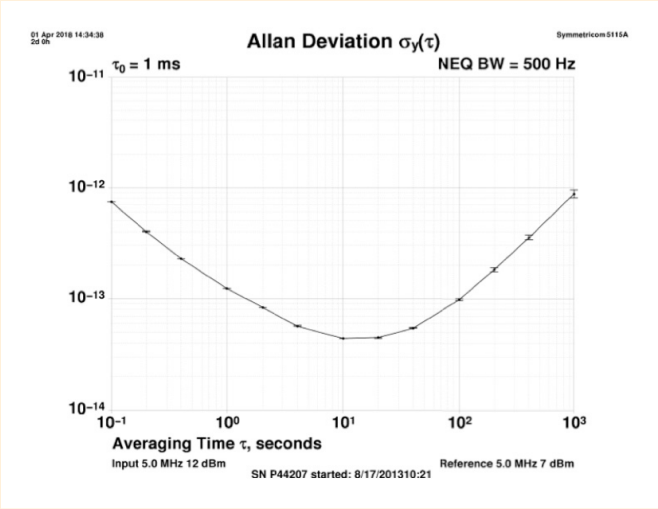

Figure 3. Allan Deviation of the SMA iMaser measured against the SC-11 crystal oscillator on loan from Johns Hopkins Applied Physics laboratory. Both the maser and the crystal were in fine form for the EHT campaign, as evidenced by the Allan Deviation substantially lower than 1e-13 between 1 and 100 seconds.

Figure 4. During a schedule gap, the crew for the first few nights ham it up in the correlator room with the 64 Gbps SWARM. From right to left: Jennie Berghuis, Miriam Fuchs (SMA Operators), André Young and Jonathan Weintroub. We benefitted also from the expert services of other operators, including Ryan Howie and Andrew Weis. Despite retiring a full month before, Taco kindly provided foundational support from Cambridge.

pling of the signal, and transformation of that signal back to the time-domain is also required prior to correlation with data from other EHT stations. Finally, the output data have to be properly formatted according to the VDIF (VLBI Data Interchange Format) standard.

This interpolation and inversion to time series is currently in process using the "Adaptive Phased Array Heterogenous Interpolating Downsampler for SWARM" (APHIDS) pre-processor. APHIDS runs on a General-Purpose Graphics Processing Unit (GP-GPU). The algorithm uses Fourier-interpolation, transforming between the time- and frequency-domains with windows of appropriate size to effect a net downsampling rate of 4576/4096 = 143/128.

SMÖRGÅSBORD: MASER, JCMT, STAFFING, AND CURRENT WORK

The JCMT for the first time functioned as an independent VLBI station, referenced to the SMA maser but with its own reference generator designed and installed in the SMA vault by Derek Kubo and Paul Yamaguchi. Thus the JCMT can be provided with a maser locked reference signal without using IF/LO equipment used for one of the SMA antennas; and, the JCMT can be supported without sacrificing the collecting area of a single SMA antenna. We verified fringe coherence to the JCMT each night before operations, which went very smoothly, and actually worked the first time we tried it. The SMA maser is performing excellently for the campaign and generally, as shown in figure 3.

The data are split into high and low bands, each of 2 GHz bandwidth with two bands per polarization. The VLBI correlators at MIT Haystack Observatory and at the Max Planck Institute for Radioastronomy in Bonn will process the low and high bands respectively for all stations. All disk modules were shipped and have been received at the processing centers except for those that remain at the South Pole. The South Pole modules will be shipped when the station opens in October and will be correlated starting in November 2018.

Dr. Alex Raymond joined SAO as a postdoc in June and is working on developing an FPGA-based real-time version of APHIDS, which will enable recording VLBI correlation-ready data directly at the summit during an observation. The hardware platform for this application is the SKARAB, built around the Xilinx Virtex 7 FPGA. This continues the earlier work of intern Mark Peryer.

A diverse multi-wavelength network observed SgrA*, M87 and other AGN along with the EHT. As the EHT data processing progresses, we will keep in close touch with our multi-wavelength colleagues for joint analysis. With the EHT hitting its target bandwidth of 64 Gbps we are entering an exciting era both for the EHT, and the SMA's participation in it as a mainstay.

TACO RETIRES: 22 YEARS OF EXCEPTIONAL SERVICE

Jim Moran (SMA Director, 1995 – 2005)

Taco retired on his 60th birthday, February 27, 2018. A foundational mainstay of the SMA, esteemed by all, he will truly be missed. His life was built around the SMA and he was literally always on duty in support of it 24 hours a day. He had intimate knowledge of virtually every aspect of the instrument and as his annual review in 2006 put it succinctly: "he is willing to help anyone at any time."

Taco was born and grew up in Des Moines, Iowa. He acquired the name "Taco" when he was in high school and worked in a Mexican restaurant. Later he took on the alias "Raoul Taco Machilvich" and his email address was RTM@cfa. The local folklore has it that RTM alternatively stands for "Read the Manual", a sly second meaning that is entirely typical of Taco's sense of humor. Taco attended Carleton College where he majored in both physics and mathematics. He entered graduate school at Caltech in 1980 but took a four year break starting in 1983 to work full time for the CSO doing the real-time programming, installing hardware and firmware, pulling many miles of cable, and working on commissioning the telescope. He returned to his graduate studies in 1987 and finished with a thesis entitled "Submillimeter and Infrared Observations of Mass Lost by AGB Stars" under Tom Phillips, which was based mainly on CSO observations. Evolved stars were to remain as his primary scientific focus for the rest of his career. In 1993 he became the chief resident programmer at the CSO. Then in 1996, he decided he wanted a new challenge and was hired by the SMA to lead the real-time programming, a position he held until his retirement. Tom Phillips rued about his lot in life being to train astronomers for other people's observatories. Although Taco was seeking a new challenge, he cited one of the reasons he moved from Hawaii was that he could not stand the chirping of the coqui, an invasive species from Puerto Rico.

Taco's job description included the task "work with the online group to design, develop, integrate and document the online portion of the SMA software." Upon his arrival, the software

development lacked an overall guiding vision. There were three CPU types, two real-time operating systems, and two bus architectures. Within a year Taco had completely reorganized the system around a single CPU, operating system, and bus architecture. About a decade later, in a very uncharacteristic boast, Taco remarked that none of the original code survived his redesign! He went on to write the code for the correlator control, and later the custom code for the e-SMA (operations with the CSO and JCMT), and the new SWARM correlator introduced in 2015. Taco organized much of the SMA testing and commissioning program, and became the primary expert in making the SMA run.

Taco had a wry and playful sense of humor. Much of it is preserved for posterity on the log of dialog between the telescope operators and support staff recorded on the program "2op". His own contributions take up 5 Mbytes of disk space. Some gleanings from the 2op include flippant remarks such as: "More and more Americans are switching to the SMA as their ISP (Interferometry Service Provider) just to get access to SMA instant messaging," and "… Actually, Venus might be better. It's a little further from the Sun, and much stronger. Plus, it's no fun observing Mercury when Ant isn't around." He would do his utmost to wind Ant up by performing remote observations from his Palm Treo when links to the observatory from a roaming Treo were not that reliable.

For his entire 22 year career at SAO, he lived in an apartment on Walden Street in Cambridge within an easy walking distance of the observatory. He was often seen walking to his apartment in his characteristic pith helmet. He would never accept a ride.

Taco always spoke softly and his kind demeanor endeared him to everyone he came in contact with. He was known for his incredible politeness and patience. He was never too busy to explain things to people. No matter where he was, he was rarely off-line, always cheerfully willing to help solve any problem with the SMA, day or night. In fact, there has never been a documented case where someone called on Taco and found him to be asleep.

Taco had a fascination with Iran and Persian culture. He learned to write Farsi in cursive script and read Persian poetry in his spare time. Taco really enjoyed Thai and South Indian food. He usually instructed restaurant waiters to make his order as spicy as possible. Otherwise, he subsisted mostly on junk food. When someone asked him why he often carried around a bag of oranges, he replied that it was to ward off scurvy. Staples included Hostess HoHos, Goldfish crackers, and Peeps (a sugary marshmallow based junk food). His love of chocolate is well documented on the log entries. Regarding dinners at Hale Pohaku Taco said: "it is your duty to eat what is proffered so that it will not appear on the lunch menu the next day."

For many years Taco distributed Christmas presents based on his own designs to all the SMA staff. Items included T-shirts and sweatshirts displaying the SAO pad layouts, mugs, water bottles, and one year a Leatherman tool embossed with the SMA logo. The first T-shirt had the wonderful front/back split: the front was "SMA Hawaii" with a lovely picture of the SMA in Hawaii - the back depicted "SMA Cambridge" with an image of a montage of Federal forms and paperwork. In designs he made of the array layout, he christened the hill on which Subaru sits as "Beacon Hill," a nod to both the Boston landmark and the site of the holography transmitter.

Taco really knew the lore of the nighttime sky. He thought professional astronomers had a disturbing lack of knowledge of the sky. He always enjoyed pointing out many wonderful naked eye and small telescope objects. He created the instantaneous control monitor display, known as "orrery", of the full sky labeled with many celestial landmarks as well as the current target of the SMA. A click on the sun icon produced the comment: "Point the array at the sun and you won't leave this island alive". He proudly displayed his membership certificate in the American Association of Variable Star Observers on his wall. He was also a great fan of total solar eclipses. Last year he went to Iowa to meet up with his mom to view the great American eclipse. Unfortunately, it rained and they missed it!

Taco was a great hiker. He often preferred to walk from Hale Pohaku to the summit of Maunakea. He led hikes to Pu'u O'o and the active lava lake near it (the origin of the current lava flows), much to the consternation of the rangers. Some memorable trips on the Big Island produced singed hairs and melted shoe soles.

Taco enjoyed the long road trips home (Iowa) every Christmas. He would try to do them with as little break as possible. It would be wonderful if he could drive back to visit us.

Todd Hunter, Jill Knapp, Colin Masson and SMA Staff contributed to this article.

First Fringes in Hawaii. From left to right: Martina Wiedner, T K Sridharan, Bill Snow, Nimesh Patel, Edward Tong, Ray Blundell, Charlie Katz, Todd Hunter, Matt Dexter and Taco.

The first-light two-element interferometric fringes were obtained with the first pair of SMA antennas operating at 230 GHz on Maunakea using an analog correlator and a chart. The source observed was Saturn, and the time was around 9 hours UTC, 30 September 1999. The fringes were recorded on our trusty analog chart recorder that Bob Wilson had brought from Bell Labs. The next night, spectral line fringes were obtained on the CO(2-1) line in Orion with the SMA's digital correlator. This picture was probably taken by Ant Schinckel, who was definitely there at the time. Earlier, fringes at 230 GHz were obtained at the fabrication and test center (MIT Haystack) on 23 October 1998.

Receiver Lab. From left to right: Ray Blundell, Scott Paine, Edward Tong, Taco and Todd Hunter.

A visit by former SMA receiver lab scientist, Todd Hunter, just before Taco retired that led to an impromptu luncheon at the favorite haunt of the receiver lab: John Harvard's Brewery and Ale House.

Ant Schinckel (Director of Hawaii Operations 1998 – 2007) and Taco

I first met Raoul Taco Machilvich, alias Ken Young, in 1988 when I moved from the DC wavelengths of radio astronomy at the 100-m at Effelsburg to Tom Phillips' submillimetre group at Caltech, then in the process of building the Caltech Submillimetre Observatory (CSO) on Maunakea.

Taco had of course been instrumental in getting the CSO going, doing not only software but many miles of cabling installation and pieces of miscellaneous hardware and firmware. We spent many long nights at CSO getting new observing modes going, Taco slaving over the VT100 terminals editing Forth in the RT computers, and me usually acting as the observer in the sidecar (or top floor) to see if the new mode moved things in the expected way. We had some amusing incidents - when the control board for a stepper motor drive was unfortunately damaged so the leg from one pin on an IC was severed and Taco and I decided there was nothing to lose by grinding the chip away to expose where the lead went inside and then soldering it back: successfully I might add! In the traditional manner, when this stepper motor board was finally replaced, he and I disposed of it in an appropriate way that involved the Gemini telescope. Many of our evenings at the CSO were spent in deep political arguments as we did not quite agree in this domain (polar opposites) - but they always remained totally non-acrimonious.

Taco spent many evenings at the CSO with different observers - Annelia Sargent and Nick Scoville and many others from Caltech and Texas. But Gary Melnick and Karl Menten were two of the most prolific early users of the facility and Taco and Karl, in particular, had competitions to see who could consume the most junk food. I don't know if the Hostess HoHos or the Peeps won out but I had more than one reason to never join the competitions. Apparently, expiration dates were considered a "suggestion" because the dried Peeps that sat in Taco's office could be used to write on the chalkboard. This along with the sugar-level dissuaded me from ever trying one.

After his sense of humor, I think the thing I remember most about Taco was his incredible politeness, patience, and generosity. Taco was never too busy to explain things that you didn't understand - he was infinitely patient at explaining the submillimeter world to me, and later, the night sky to my partner Laurie when she started working giving tours on Maunakea, showing her the highlights of what could be seen in a C8.

From Jill Knapp (Professor of Astrophysics, Princton University)

I was very fortunate to be in on the very early days of the CSO, observing extensively with Taco, taking data with CSO as part of the commissioning. My strongest recollections of Taco are related to the effect on one's behavior while working at the high-altitude (13,803') on Maunakea. Many people get sick, many get very grumpy: Taco and I both got unbearably silly and were in more or less constant fits of helpless laughter. Those of you who know Tom Phillips know that he has a wide repertoire of eloquent sighs. He would call-in as we were setting up at sunset to find out how the tests and commissioning were going and to suggest further things to do. Taco would report, there would be a couple of seconds' silence, then a long sigh from Tom. We entertained ourselves during long integrations by constructing a device for measuring the azimuth, to wit, a Foucault pendulum - the CSO dome, inside of which is the observing room, rotates with the telescope. We even wrote an operating manual for it.

Taco is a fearless driver, and stories of Taco's driving escapades abound. I was **very** glad it was him behind the wheel on those nights when bad weather forced us down the mountain, and one time he barrelled right through a large snowbank blocking the road out of the CSO parking area. We were called up from Hale Pohaku one night, and told to get down and to convoy with the JCMT crew. We went to look out of the exit door from the dome to see what was happening and I made the mistake of stepping outside and was blown away. I can still see Taco at the door, waving a flashlight into the darkness and shouting, "Jill? Jill??" as I sailed along on my back on the ice.

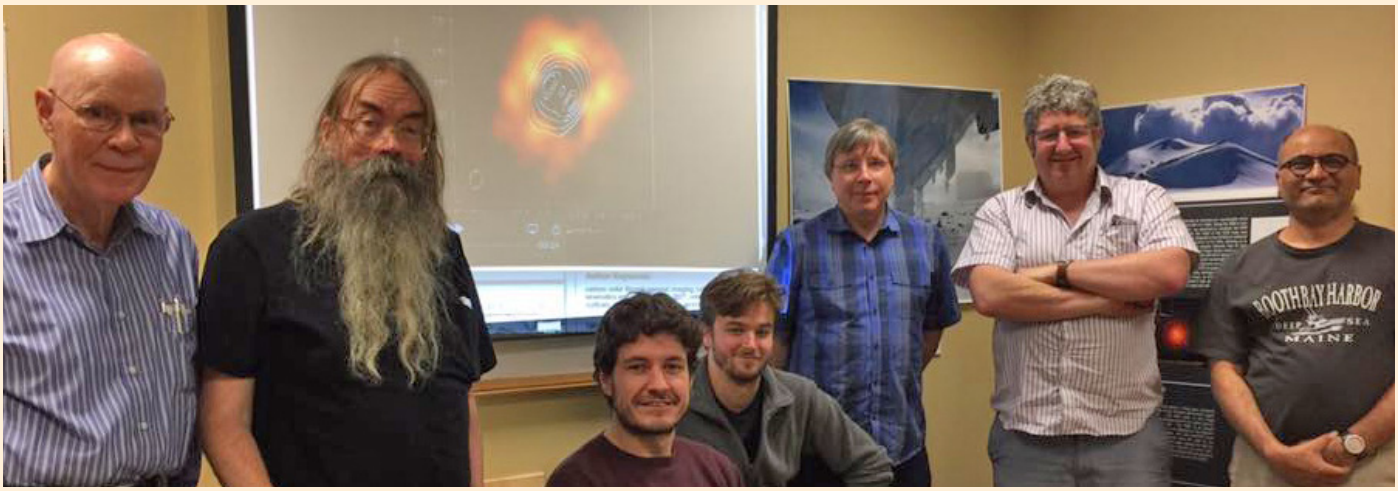

SWARM Team. From left to right: Bob Wilson, Taco, André Young, Rurik Primiani, John Test, Jonathan Weintroub and Nimesh Patel.

The first part of SWARM's development involved choosing hardware and building on CASPER's designs to make a wideband correlator. But, of course to be useful, it had to work with the SMA's real-time systems. Taco eagerly stepped in, gently explained how SWARM should fit in, made the required modifications to the realtime system and tested repeatedly as the two systems were successfully brought together.

From Colin Masson, Sr. SMA Scientist (1989–1995) I had the good fortune to work with Taco at several observatories. My introduction to his skill and sense of humor came at OVRO where he created a network (Taconet) to link the computers together. The principal operations were getting and sending files, or spooling them to the printer. So the respective commands were "suck", "spit" and, of course, "drool".

Taco was enthusiastic about driving. For example, when he arrived in LA, he made a point of driving over every piece of freeway in the area.

At CSO, Taco was critical to the development and operation of the Observatory and he was always helpful to others. When a question arose at any time of day or night in any time zone, he always seemed to be awake and ready to log in and help out.

This picture is from SMAOC Log #8780: "Here is a photo of our software leader trying to dislodge ice from the correlator AC duct. This action is required before correlator software work can resume after snowy weather. If someone spent a day and rigged up a simple three-sided sheet metal shroud, I believe his time could be spent more profitably for the project."

Todd Hunter, SMA, Postdoctoral fellow (1996-1999), Astrophysicist (1999-2006)

I had the great privilege of overlapping with Taco first as a fellow grad student at Caltech. I learned practical programming skills for synchronizing actual hardware and various servers by emulating his CSO control code. We later occupied adjacent offices in Cambridge where he continued to teach me more advanced skills like threads, semaphores, and RPC. During some tests we would communicate between our respective workstations by shouting! Regarding the SMA, no task was beneath him.

Some excerpts from the 2op (operator communications log).

```
Thu 02:46:18 (rtm) More and more americans are switching to the SMA as
Thu 02:46:35 (rtm) their ISP (Interferometry Service Provider) just to
Thu 02:46:47 (rtm) get access to SMA instant messaging.

Thu 02:41:45 (rtm) It is kinda cute that it prints every digit in a
Thu 02:42:06 (rtm) 230 digit floating point number.   Gottat respect
Thu 02:42:26 (rtm) that kind of faith in IEEE double precision.

Fri 06:11:29 (rtm) You can COUNT on evolved stars, unlike those flakey
Fri 06:11:40 (rtm) young stellar objects.

Thu 09:49:00 (rtm) Better to eat junk food, than collect junk data.

Wed 08:18:08 (rtm) Today it sounded like Charlie wanted to delay the test.
Wed 08:18:31 (rtm) Apparently the comet is a real wimp, and there's no chance
Wed 08:19:10 (rtm) we'll be able to see if the new software works on such a
Wed 08:19:16 (rtm) loser of a comet.

Mon 20:16:46 (rtm) It means warm.
Mon 20:19:16 (rtm) Actuall, Venus might be better.
Mon 20:19:30 (rtm) It's a little further from the Sun, and much stronger.
Mon 20:20:02 (rtm) Plus, it's no fun observing Mercury went Ant isn't around.

Wed 12:41:14 (rtm) 3C 454.3 is pretty strong, but it will be near transit
Wed 12:41:37 (rtm) when Sgr A* surrenders to Poliahu's embrace.

Thu 03:55:04 (rtm) On nights like this, Lake Waiau turns to chocolate.

Sat 02:08:49 (rtm) That's how I got my chocolate covered expresso bean
Sat 02:08:49 (rtm) addiction.

Fri 05:11:36 (rtm) It is happy in the land of choclate lakes and gumdrop
Fri 05:11:36 (rtm) mountains.

Thu 09:39:48 (rtm) It varies with (1/r)^4, where r is the distance between
Thu 09:39:57 (rtm) the chocolate and my mouth.
Thu 09:43:08 (rtm) So you're expecting a variety of Big Island Candy treats?

Thu 09:45:05 (rtm) There is no need to fatten me further.
Thu 09:45:44 (rtm) They already adjust the airline baggage depending on my
Thu 09:45:51 (rtm) seat assignment.

Thu 02:04:58 (rtm) Chocolate is for closers.

Sun 12:48:28 (rtm) So you just like torturing your co-workers at the summit,
Sun 12:48:28 (rtm) with rumors of chocolate?

Wed 08:34:20 (rtm) I was never bored for a second in LA.
Wed 08:34:41 (rtm) Sweet, smoggy dreams.
Wed 08:36:54 (rtm) There are places in LA county that are far more
Wed 08:36:54 (rtm) inaccessible, and have more wild fauna, than anywhere I've
Wed 08:36:54 (rtm) run across in Hawaii.

Wed 08:25:27 (rtm) I lived there for 3 years.   Towards the end, I was spending
Wed 08:25:27 (rtm) all my money flying to LA every weekend.   I'd arrive in LA
Wed 08:25:27 (rtm) so trashed that I just slept in a hotel until I had to fly
Wed 08:25:27 (rtm) back.   It was *still worth it*.
```

Shelbi Hostler Schimpf, Telescope Operator/2nd Shift Coordinator. As a summit operator, it was always a pleasure to see the message come over 2op: "How are things on the dusty bump?" Taco seemed to have a sixth sense of when he was needed, as fairly often he would check in right around the time we were at the "Call Taco" step in our troubleshooting (of course that was most likely due to emails or alerts he was receiving from systems being out of whack or rebooted). Summit shifts with Taco were particularly enjoyable, because not only was it an incredible learning experience, but if one made a comment or suggestion about software or a display, chances were he would edit the code and implement the change immediately. It was always a joy to see Taco on his visits to Hilo, for everyone from SMA staff to the cooks at HP. Since transferring to Cambridge in 2010, I have not yet had a trip to HP where fewer than 3 HP staff members have asked about Taco, and sent back their well wishes.

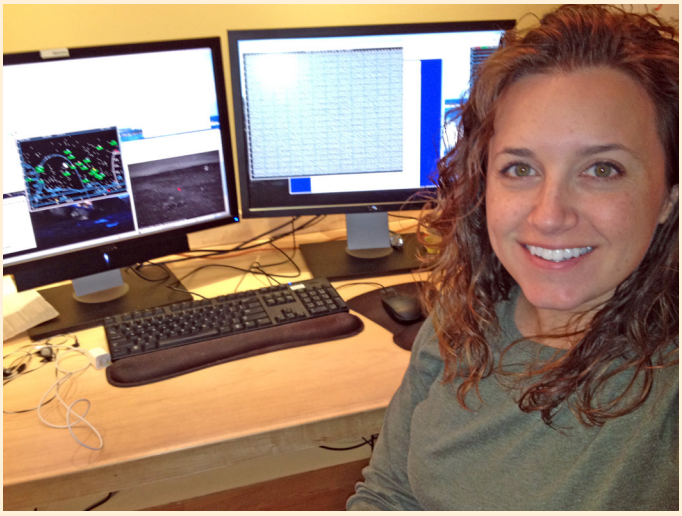

STAFF CHANGES IN HILO

Carolyn Ridderman, Administrative Assistant, left the SMA at the end of April to move to the mainland. We thank Carolyn for her efforts and wish her success in the future.

Solomon Ho, Electronics Technician, joined SAO in May, reporting to John Maute. Previously he worked at the YTLA on Maunaloa.

Naomi Owens, Computing/Network Specialist, joined ASIAA in May. Previously she worked at the Hawaii Department of Education.

SMA POSTDOCTORAL FELLOWS: COMINGS AND GOINGS

The Submillimeter Array Postdoctoral Fellowship program supports young scientists active in a variety of astronomical research fields involving submillimeter astronomy. The SMA Fellowship is competitive, and a high percentage of our past Fellows have gone on to permanent faculty and research staff positions located around the world.

The SMA welcomes our newest Fellow: **Andrew Burkhardt.**

Andrew is completing his PhD research at the University of Virginia with the thesis "Constraining Ice-mantle and Gas-phase Astrochemistry in Regions with Shocks" (Advisor: Tony Remijan, NRAO/Uva), focused on constraining the roles and interplay between grain-surface and gas-phase chemistry through the synthesis of single-dish and interferometric radio observations and chemical network models, including the role of shocks, molecular families with multiple formation routes, isotopologue chemistry, and dust-grain precursors.

Andrew joins continuing SMA Fellows Tomasz (Tomek) Kaminski, Garrett (Karto) Keating, Luca Matrà, and Maria Jesus Jimenez-Donaire.

As new Fellows arrive, we also take the time to thank those Fellows who are moving on to even bigger things:

Dr. Shaye Storm has accepted employment as a Research Analyst for the CNA Corporation's Center for Naval Analyses. The Center for Naval Analyses is a Federally Funded Research and Development Center (FFRDC) located in Arlington, Virginia. We wish Shaye (and all our current and former Fellowship holders) contined success!

A list of current and former SMA Fellows is provided at https://www.cfa.harvard.edu/opportunities/fellowships/sma/smafellows.html along with further information on the SMA Fellowship program. Applications for the 2018 SMA Fellowships were due in October 2017. We anticipate the deadline for the 2019 SMA Fellowship opportunities will be in October 2018.

Mark A. Gurwell
Chair, SMA Fellowship Selection Committee

POSTDOCTORAL OPPORTUNITIES WITH THE SMA

Applications for the 2019 Submillimeter Array (SMA) Postdoctoral Fellowship program will be due in fall 2018. We anticipate offering one or more SMA Postdoctoral Fellowships starting Summer/Fall 2019.

The SMA is a pioneering radio interferometer designed for arc-second imaging in the submillimeter spectrum. SMA science spans an impressive array of fields, ranging from our solar system, through imaging of gas and dust and tracing magnetic fields in stellar nurseries and planet-forming disks, to exploration of nearby galaxies and imaging of dusty star-forming galaxies at high redshift. In addition to its outstanding record in astronomical research, the SMA is a world leader in the design of wide-bandwidth, high-frequency radio receivers for astronomy. The SMA recently commissioned a next generation correlator which vastly increases total bandwidth (to 8 GHz/sideband per polarization) while retaining high spectral resolution (140 kHz) across the entire processed spectral range, providing significantly enhanced science capability, and further expansion to 12 GHz/sideband per polarization is underway.

These positions are aimed chiefly at research, both observational and theoretical, in submillimeter astronomy. Successful candidates will participate in remote and on-site observations with the SMA, research in their interpretation, and/or instrument development. While the SMA fellowships are intended primarily for research associated with the SMA, our main offices at the Center for Astrophysics provide Fellows with unique opportunities to develop collaborations within the wider CfA community and enjoy extraordinary freedom in structuring their research activities. Applicants must have a recent Ph.D. in astronomy or a related field.

The SMA is a collaboration between the Smithsonian Astrophysical Observatory and the Academia Sinica Institute of Astronomy and Astrophysics in Taipei, Taiwan. The Smithsonian Astrophysical Observatory is an Equal Opportunity/Affirmative Action Employer where all qualified applicants receive equal consideration without regard to race, color, creed, national origin or gender.

Application information and instructions can be found at:

http://www.cfa.harvard.edu/opportunities/fellowships/sma

The deadline for applications has not yet been determined but is expected to be in early October 2018. Please check the above link for up to date information on the deadline and application procedure.

Questions: smapostdoc@cfa.harvard.edu

CALL FOR STANDARD SMA OBSERVING PROPOSALS- 2018B SEMESTER

The SMA invites standard observing proposals from the world wide astronomical community for the 2018B semester with observing period Nov 16, 2018 - May 15, 2019. The proposal deadline is 06 September 2018. The SMA Observer Center (http://sma1.sma.hawaii.edu) is expected to open for proposal submission on 14 August 2018.

The SMA is a reconfigurable interferometric array of eight 6-m antennas on Maunakea jointly built and operated by the Smithsonian Astrophysical Observatory and the Academia Sinica Institute of Astronomy and Astrophysics. The array operates in the 230, 345 and 400 GHz bands.

The SMA has recently completed significant upgrades in observational capability, with more under way. Currently, the SMA observes simultaneously with two orthogonally polarized receivers, one in the 230 GHz or 345 GHz band and the other in the 240 GHz or 400 GHz band (with full polarimetric observations available using the 230+240 or 345+400 band combinations). The SWARM correlator processes 8 GHz bandwidth for each receiver in each sideband, for a total of 32 GHz, at a uniform 140 kHz resolution. This 32 GHz frequency coverage can be continuous where the tuning ranges overlap for the two orthogonally polarized receivers. In short, the SMA now provides flexible, wide band frequency coverage that delivers high continuum sensitivity and excellent spectral line capabilities. A full track offers continuum sensitivity of 200 or 500 micro-Jy (1 sigma) at 230 or 345 GHz in good weather conditions (precipitable water vapor 2.5mm and 1.0mm, respectively). The corresponding line sensitivities at 1 km/s resolution are 30 and 70 mJy. The small antennas allow access to low spatial frequencies in the sub-compact configuration, and at the other extreme, the finest angular resolution with the very extended configuration at 345 GHz is ~ 0.25". The compact and extended configurations complete the range. Thus, in some ways, the characteristics and performance of the SMA are both similar and complementary to those of the stand-alone Atacama Compact Array (ACA) component of ALMA. For more information about SMA capabilities, visit the SMA Observer Center website (http://sma1.sma.hawaii.edu/status.html) and explore the set of SMA proposing tools (http://sma1.sma.hawaii.edu/tools.html). Current and archived SMA Newsletters available online (https://www.cfa.harvard.edu/sma/newsletter/) provide a sampling of the wide variety of science possible with the SMA.

STANDARD OBSERVING PROPOSALS

Submissions open: **14 August 2018** (expected date)
Submissions close: **06 September 2018**

LARGE SCALE PROJECTS PROPOSALS

Notice of Intent: **02 July, 2018** (Closed)
Full submission: **09 August, 2018**

For more details visit the following websites:

General - http://sma1.sma.hawaii.edu/proposing.html
Large Scale Projects - http://sma1.sma.hawaii.edu/call_largescale.html
Notice of Intent - http://sma1.sma.hawaii.edu/legacysubmit.html

Questions or comments regarding the Call for Large Scale Proposals can be addressed to sma-largescale@cfa.harvard.edu and on standard proposals to sma-proposal@cfa.harvard.edu.

T. K. Sridharan
Chair, SMA Time Allocation Committee

PROPOSAL STATISTICS 2018A (16 MAY 2018 – 15 NOV 2018)

The SMA received a total of 77 proposals (SAO 58) requesting observing time in the 2018A semester. The proposals received by the joint SAO and ASIAA Time Allocation Committee are divided among science categories as follows:

Category	Proposals
high mass (OB) star formation, cores	28
local galaxies, starbursts, AGN	12
low/intermediate mass star formation, cores	10
submm/hi-z galaxies	6
GRB, SN, high energy	5
protoplanetary, transition, debris disks	5
evolved stars, AGB, PPN	3
UH	3
Galactic center	1
large scale projects	1
Other	1
solar system	1
ToO/DDT	1

TRACK ALLOCATIONS BY WEATHER REQUIREMENT (ALL PARTNERS):

PWV[1]	SAO	ASIAA	UH[2]
< 4.0mm	37A + 42B	13A + 9B	11
< 2.5mm	28A + 25B	6A + 6B	4
< 1.0mm	0A + 0B	0A + 0B	0
Total	**65A + 67B**	**19A + 15B**	**15**

(1) Precipitable water vapor required for the observations.

(2) UH does not list As and Bs.

TOP-RANKED SAO AND ASIAA PROPOSALS – 2018A SEMESTER

The following is the listing of all SAO and ASIAA proposals with at least a partial A ranking with the names and affiliations of the principal investigators.

EVOLVED STARS, AGB, PPN

(NOTE: CONTINUATION OF 2017B PROJECT)

Tomasz Kaminski, CfA, SMA fellow
Chemical and isotopic composition of the stellar-merger remnant, CK Vul

GALACTIC CENTER

Tomoharu Oka, Department of Physics, Faculty of Science and Technology, Keio University
*Search for Intraday Flux Variation of the Intermediate-mass Black Hole Candidate CO-0.40-0.22**

GRB, SN, HIGH ENERGY

Alexandra Tetarenko, University of Alberta
Constraining Jet Formation and Evolution with Transient X-ray Binaries

Kuiyun Huang, CYCU
New Insights in Short GRBs

Yuji Urata, NCU
Search for Bright submm GRB afterglows Toward Radio Polarimetry

HIGH MASS (OB) STAR FORMATION, CORES

Shaye Storm, SAO
Forming the NGC 6334 Filament: Shocked Gas and Searching for Outflows

Shih-Ping Lai, National Tsing Hua University, Taiwan
Pilot mosaic polarization observations towards W51 and Orion BN/KL

Sihan Jiao, National Astronomical Observatories, Chinese Academy of Sciences
Continuation of SMA Public Survey towards the Orion Molecular Cloud

LARGE-SCALE PROJECTS

Jan Forbrich, University of Hertfordshire and
Charles Lada, SAO
SMA Survey of Resolved Dust and Simultaneous CO Observations of GMCs in M31

LOCAL GALAXIES, STARBURSTS, AGN

Erin Kara, University of Maryland
Testing the radio-jet / X-ray corona connection in a unique Gamma-ray Loud Seyfert

LOW/INTERMEDIATE MASS STAR FORMATION, CORES

Anaelle Maury, CEA, Paris Saclay University, Astrophysics department
Evidence of magnetic braking in Class 0 protostars : towards a statistical view

Yusuke Aso, Academia Sinica Institute of Astronomy and Astrophysics
Pilot Survey of Deuterated Molecules in Class 0 Protostars

PROTOPLANETARY, TRANSITION, DEBRIS DISKS

Luca Matrà, Harvard-Smithsonian Center for Astrophysics
REsolved ALMA and SMA Observations of Nearby Stars (REASONS): a legacy population study of the formation location of planetesimal belts (part 2)

SOLAR SYSTEM

Alain Khayat, NASA Goddard Space Flight Center and the University of Maryland
Characterizing the physical state of the Martian atmosphere during a global dust storm

TOO/DDT

Anna Ho, Caltech
SMA Monitoring of the Rare Relativistic Supernova AT2018cow

ALL SAO PROPOSALS – 2017B SEMESTER

The following is the listing of all SAO proposals observed in the 2017B semester (16 NOV 2017 – 15 MAY 2018).

Sean Andrews, CfA
A Pilot Study of the Size--Frequency Correlation in Protoplanetary Disks

Yusuke Aso, ASIAA
Verifying relation between kinematics and B-fields around the protostar TMC-1A

Adwin Boogert, University of Hawaii
The Origin and Location of Sulfur-bearing Molecules in Protostellar Environments

L. Ilsedore Cleeves, CfA
Characterizing X-ray driven molecular chemistry in a young protoplanetary disk

David Clements, Imperial College London
Case study of an extremely luminous, highly spatially extended starburst only 1.7Gyr after the Big Bang

Martin Cordiner, NASA Goddard Space Flight Center
Observations of the highly-unusual comet R2/PanSTARRS

Sheperd Doeleman, SAO
Event Horizon Imaging of SgrA and M87*

Jan Forbrich, CfA
Measuring resolved dust emission from individual GMCs in M31

Naomi Hirano, ASIAA
Is the L1448C(N) protostellar jet "extremely active"? -- three dimensional kinematic structure probed by proper motions

David Jewitt, UCLA
Geminid Parent (3200) Phaethon Flyby

Sihan Jiao, National Astronomical Observatories
A Pilot SMA Public Survey towards the Orion Molecular Cloud

Atish Kamble, CfA
Search for Radio Emission from Superluminous Supernova SN2017egm

Tomasz Kaminski, CfA
Chemical and isotopic composition of the stellar-merger remnant CK Vul

Tomasz Kaminski, CfA
Ay191 Course - High Resolution Observations of Outflows in a Protobinary System

Shih-Ping Lai, National Tsing Hua University
Pilot mosaic polarization observations towards W51 and Orion BN/KL

Tsz Kuk Daisy Leung, Cornell University
Excitation of the star-forming gas in a strongly-lensed wet-merger at z~0.65

Luca Matrà, CfA
REsolved ALMA and SMA Observations of Nearby Stars (REASONS): a legacy population study of the formation location of planetesimal belts

Karin Öberg, Harvard University
Resolving HCN in five Taurus protoplanetary disks

Iván Oteo Gómez, University of Edinburgh / ESO
Resolving the ISM of low-z submm galaxies

Glen Petitpas, CfA
Gas Properties of the Spiral Galaxy M51 and Companion.

Thushara Pillai, MPIfR
Magnetic Fields in the Cold Dense Component of Spiral Galaxies

Charlie Qi, CfA
Activity in an Ultra-Distant Long-Period Comet

Keping Qiu, Nanjing University
Mapping outflows around cold quiescent and fragmenting massive dense cores

Howard Smith, CfA
Understanding How a Black Hole Feeds: SMA Observations of SgrA Simultaneous with Keck AO*

Alexandra Tetarenko, University of Alberta
Constraining Rapid Millimeter Frequency Variability in Black Hole X-ray Binaries

Yuji Urata, NCU
Search for Bright submm GRB afterglows Toward Radio Polarimetry

Jonathan Williams, University of Hawaii
The kilo-au environment of protoplanetary disks

Ka Tat Wong, IRAM
Probing the Complex Circumstellar Environment of IRC+10420

Al Wootten, NRAO
Localization of Interstellar CH2D+: Deuteration in warm conditions

RECENT PUBLICATIONS

Title: A Magnetic Field Connecting the Galactic Center Circumnuclear Disk with Streamers and Mini-spiral -Implications from 850 μm Polarization Data
Authors: Hsieh, Pei-Ying; Koch, Patrick M.; Kim, Woong-Tae; Ho, Paul T. P.; Tang, Ya-Wen; Wang, Hsiang-Hsu
Publication: *eprint arXiv:1806.02719*
Publication Date: 06/2018
Abstract: http://adsabs.harvard.edu/abs/2018arXiv180602719H

Title: Detection of Intrinsic Source Structure at ~3 Schwarzschild Radii with Millimeter-VLBI Observations of SAGITTARIUS A*
Authors: Lu, Ru-Sen; Krichbaum, Thomas P.; Roy, Alan L.; Fish, Vincent L.; Doeleman, Sheperd S.; Johnson, Michael D.; Akiyama, Kazunori; Psaltis, Dimitrios; Alef, Walter; Asada, Keiichi; Beaudoin, Christopher; Bertarini, Alessandra; Blackburn, Lindy; Blundell, Ray; Bower, Geoffrey C.; Brinkerink, Christiaan; Broderick, Avery E.; Cappallo, Roger; Crew, Geoffrey B.; Dexter, Jason; Dexter, Matt; Falcke, Heino; Freund, Robert; Friberg, Per; Greer, Christopher H.; Gurwell, Mark A.; Ho, Paul T. P.; Honma, Mareki; Inoue, Makoto; Kim, Junhan; Lamb, James; Lindqvist, Michael; Macmahon, David; Marrone, Daniel P.; Martí-Vidal, Ivan; Menten, Karl M.; Moran, James M.; Nagar, Neil M.; Plambeck, Richard L.; Primiani, Rurik A.; Rogers, Alan E. E.; Ros, Eduardo; Rottmann, Helge; SooHoo, Jason; Spilker, Justin; Stone, Jordan; Strittmatter, Peter; Tilanus, Remo P. J.; Titus, Michael; Vertatschitsch, Laura; Wagner, Jan; Weintroub, Jonathan; Wright, Melvyn; Young, Ken H.; Zensus, J. Anton; Ziurys, Lucy M.
Publication: *The Astrophysical Journal, Volume 859, Issue 1, article id. 60, 11 pp. (2018). (ApJ Homepage)*
Publication Date: 05/2018
Abstract: http://adsabs.harvard.edu/abs/2018ApJ...859...60L

Title: The 1.4 mm core of Centaurus A: First VLBI results with the South Pole Telescope
Authors: Kim, Junhan; Marrone, Daniel P.; Roy, Alan L.; Wagner, Jan; Asada, Keiichi; Beaudoin, Christopher; Blanchard, Jay; Carlstrom, John E.; Chen, Ming-Tang; Crawford, Thomas M.; Crew, Geoffrey B.; Doeleman, Sheperd S.; Fish, Vincent L.; Greer, Christopher H.; Gurwell, Mark A.; Henning, Jason W.; Inoue, Makoto; Keisler, Ryan; Krichbaum, Thomas P.; Lu, Ru-Sen; Muders, Dirk; Müller, Cornelia; Nguyen, Chi H.; Ros, Eduardo; SooHoo, Jason; Tilanus, Remo P. J.; Titus, Michael; Vertatschitsch, Laura; Weintroub, Jonathan; Zensus, J. Anton
Publication: *eprint arXiv:1805.09344*
Publication Date: 05/2018
Abstract: http://adsabs.harvard.edu/abs/2018arXiv180509344K

Title: The Millimeter Continuum Size-Frequency Relationship in the UZ Tau E Disk
Authors: Tripathi, Anjali; Andrews, Sean M.; Birnstiel, Tilman; Chandler, Claire J.; Isella, Andrea; Perez, Laura M.; Harris, Robert J.; Ricci, Luca; Wilner, David J.; Carpenter, John M.; Calvet, Nuria; Corder, Stuartt. A.; Deller, Adam T.; Dullemond, Cornelis P.; Greaves, Jane S.; Henning, Thomas; Kwon, Woojin; Lazio, T. Joseph W.; Linz, Hendrik; Testi, Leonardo
Publication: *eprint arXiv:1805.06457*
Publication Date: 05/2018
Abstract: http://adsabs.harvard.edu/abs/2018arXiv180506457T

Title: Detection of 40-48 GHz dust continuum linear polarization towards the Class 0 young stellar object IRAS 16293-2422
Authors: Liu, Hauyu Baobab; Hasegawa, Yasuhiro; Ching, Tao-Chung; Lai, Shih-Ping; Hirano, Naomi; Rao, Ramprasad
Publication: *eprint arXiv:1805.02012*
Publication Date: 05/2018
Abstract: http://adsabs.harvard.edu/abs/2018arXiv180502012L

Title: A masing event in NGC 6334I: contemporaneous flaring of hydroxyl, methanol, and water masers
Authors: MacLeod, G. C.; Smits, D. P.; Goedhart, S.; Hunter, T. R.; Brogan, C. L.; Chibueze, J. O.; van den Heever, S. P.; Thesner, C. J.; Banda, P. J.; Paulsen, J. D.
Publication: *Monthly Notices of the Royal Astronomical Society, Volume 478, Issue 1, p.1077-1092 (MNRAS Homepage)*
Publication Date: 07/2018
Abstract: http://adsabs.harvard.edu/abs/2018MNRAS.478.1077M

Title: MESAS: Measuring the Emission of Stellar Atmospheres at Submillimeter/millimeter Wavelengths
Authors: White, Jacob Aaron; Aufdenberg, Jason; Boley, A. C.; Hauschildt, Peter; Hughes, Meredith; Matthews, Brenda; Wilner, David
Publication: *The Astrophysical Journal, Volume 859, Issue 2, article id. 102, 6 pp. (2018). (ApJ Homepage)*
Publication Date: 06/2018
Abstract: http://adsabs.harvard.edu/abs/2018ApJ...859..102W

Title: SMA observations of the polarized dust emission in solar-type Class 0 protostars: the magnetic field properties at envelope scales
Authors: Galametz, Maud; Maury, Anaelle; Girart, Josep M.; Rao, Ramprasad; Zhang, Qizhou; Gaudel, Mathilde; Valdivia, Valeska; Keto, Eric; Lai, Shih-Ping
Publication: *eprint arXiv:1804.05801*
Publication Date: 04/2018
Abstract: http://adsabs.harvard.edu/abs/2018arXiv180405801G

Title: Submillimeter-wave emission of three Galactic red novae: cool molecular outflows produced by stellar mergers
Authors: Kaminski, T.; Steffen, W.; Tylenda, R.; Young, K. H.; Patel, N. A.; Menten, K. M.
Publication: *eprint arXiv:1804.01610*
Publication Date: 04/2018
Abstract: http://adsabs.harvard.edu/abs/2018arXiv180401610K

Title: A Search for Molecular Gas in the Host Galaxy of FRB 121102
Authors: Bower, Geoffrey C.; Rao, Ramprasad; Krips, Melanie; Maddox, Natasha; Bassa, Cees; Adams, Elizabeth A. K.; Law, C. J.; Tendulkar, Shriharsh P.; van Langevelde, Huib Jan; Paragi, Zsolt; Butler, Bryan J.; Chatterjee, Shami
Publication: *The Astronomical Journal, Volume 155, Issue 6, article id. 227, 5 pp. (2018). (AJ Homepage)*
Publication Date: 06/2018
Abstract: http://adsabs.harvard.edu/abs/2018AJ....155..227B

Title: VLBA Observations of Strong Anisotripic Radio Scattering Toward the Orion Nebula
Authors: Kounkel, Marina; Hartmann, Lee; Loinard, Laurent; Mioduszewski, Amy J.; Rodríguez, Luis F.; Ortiz-León, Gisela N.; Johnson, Michael D.; Torres, Rosa M.; Briceño, Cesar
Publication: *The Astronomical Journal, Volume 155, Issue 5, article id. 218, 5 pp. (2018). (AJ Homepage)*
Publication Date: 05/2018
Abstract: http://adsabs.harvard.edu/abs/2018AJ....155..218K

Title: Turbulence in the TW Hya Disk
Authors: Flaherty, Kevin M.; Hughes, A. Meredith; Teague, Richard; Simon, Jacob B.; Andrews, Sean M.; Wilner, David J.
Publication: *The Astrophysical Journal, Volume 856, Issue 2, article id. 117, 12 pp. (2018). (ApJ Homepage)*
Publication Date: 04/2018
Abstract: http://adsabs.harvard.edu/abs/2018ApJ...856..117F

Title: Detection of Dust Condensations in the Orion Bar Photon-dominated Region
Authors: Qiu, Keping; Xie, Zeqiang; Zhang, Qizhou
Publication: *The Astrophysical Journal, Volume 855, Issue 1, article id. 48, 8 pp. (2018). (ApJ Homepage)*
Publication Date: 03/2018
Abstract: http://adsabs.harvard.edu/abs/2018ApJ...855...48Q

Title: Discovery of an Extremely Luminous Dust-obscured Galaxy Observed with SDSS, WISE, JCMT, and SMA
Authors: Toba, Yoshiki; Ueda, Junko; Lim, Chen-Fatt; Wang, Wei-Hao; Nagao, Tohru; Chang, Yu-Yen; Saito, Toshiki; Kawabe, Ryohei
Publication: *The Astrophysical Journal, Volume 857, Issue 1, article id. 31, 8 pp. (2018). (ApJ Homepage)*
Publication Date: 04/2018
Abstract: http://adsabs.harvard.edu/abs/2018arXiv180300177T

Title: Resolved Millimeter Observations of the HR 8799 Debris Disk
Authors: Wilner, David J.; MacGregor, Meredith A.; Andrews, Sean M.; Hughes, A. Meredith; Matthews, Brenda; Su, Kate
Publication: *The Astrophysical Journal, Volume 855, Issue 1, article id. 56, 10 pp. (2018). (ApJ Homepage)*
Publication Date: 03/2018
Abstract: http://adsabs.harvard.edu/abs/2018ApJ...855...56W

Title: The Envelope Kinematics and a Possible Disk around the Class 0 Protostar within BHR7
Authors: Tobin, John J.; Bos, Steven P.; Dunham, Michael M.; Bourke, Tyler L.; van der Marel, Nienke
Publication: *The Astrophysical Journal, Volume 856, Issue 2, article id. 164, 15 pp. (2018). (ApJ Homepage)*
Publication Date: 04/2018
Abstract: http://adsabs.harvard.edu/abs/2018arXiv180208277T

Title: Radio outburst from a massive (proto)star. When accretion turns into ejection
Authors: Cesaroni, R.; Moscadelli, L.; Neri, R.; Sanna, A.; Caratti o Garatti, A.; Eisloffel, J.; Stecklum, B.; Ray, T.; Walmsley, C. M.
Publication: *Astronomy & Astrophysics, Volume 612, id.A103, 11 pp. (A&A Homepage)*
Publication Date: 05/2018
Abstract: http://adsabs.harvard.edu/abs/2018A&A...612A.103C

Title: Observational constraints on the physical nature of submillimetre source multiplicity: chance projections are common
Authors: Hayward, Christopher C.; Chapman, Scott C.; Steidel, Charles C.; Golob, Anneya; Casey, Caitlin M.; Smith, Daniel J. B.; Zitrin, Adi; Blain, Andrew W.; Bremer, Malcolm N.; Chen, Chian-Chou; Coppin, Kristen E. K.; Farrah, Duncan; Ibar, Eduardo; Michałowski, Michał J.; Sawicki, Marcin; Scott, Douglas; van der Werf, Paul; Fazio, Giovanni G.; Geach, James E.; Gurwell, Mark; Petitpas, Glen; Wilner, David J.
Publication: *Monthly Notices of the Royal Astronomical Society, Volume 476, Issue 2, p.2278-2287 (MNRAS Homepage)*
Publication Date: 05/2018
Abstract: http://adsabs.harvard.edu/abs/2018MNRAS.tmp..308H

Title: Polarization Properties and Magnetic Field Structures in the High-mass Star-forming Region W51 Observed with ALMA
Authors: Koch, Patrick M.; Tang, Ya-Wen; Ho, Paul T. P.; Yen, Hsi-Wei; Su, Yu-Nung; Takakuwa, Shigehisa
Publication: *The Astrophysical Journal, Volume 855, Issue 1, article id. 39, 19 pp. (2018). (ApJ Homepage)*
Publication Date: 03/2018
Abstract: http://adsabs.harvard.edu/abs/2018ApJ...855...39K

Title: Binary energy source of the HH 250 outflow and its circumstellar environment
Authors: Comerón, Fernando; Reipurth, Bo; Yen, Hsi-Wei; Connelley, Michael S.
Publication: *Astronomy & Astrophysics, Volume 612, id.A73, 11 pp. (A&A Homepage)*
Publication Date: 04/2018
Abstract: http://adsabs.harvard.edu/abs/2018arXiv180106939C

Title: The detection of the blazar S4 0954+65 at very-high-energy with the MAGIC telescopes during an exceptionally high optical state

Authors: MAGIC Collaboration; Ahnen, M. L.; Ansoldi, S.; Antonelli, L. A.; Arcaro, C.; Baack, D.; Babić, A.; Banerjee, B.; Bangale, P.; Barres de Almeida, U.; Barrio, J. A.; Bednarek, W.; Bernardini, E.; Berse, R. Ch.; Berti, A.; Bhattacharyya, W.; Biland, A.; Blanch, O.; Bonnoli, G.; Carosi, R.; Carosi, A.; Ceribella, G.; Chatterjee, A.; Colak, S. M.; Colin, P.; Colombo, E.; Contreras, J. L.; Cortina, J.; Covino, S.; Cumani, P.; Da Vela, P.; Dazzi, F.; De Angelis, A.; De Lotto, B.; Delfino, M.; Delgado, J.; Di Pierro, F.; Domínguez, A.; Dominis Prester, D.; Dorner, D.; Doro, M.; Einecke, S.; Elsaesser, D.; Fallah Ramazani, V.; Fernández-Barral, A.; Fidalgo, D.; Fonseca, M. V.; Font, L.; Fruck, C.; Galindo, D.; García López, R. J.; Garczarczyk, M.; Gaug, M.; Giammaria, P.; Godinović, N.; Gora, D.; Guberman, D.; Hadasch, D.; Hahn, A.; Hassan, T.; Hayashida, M.; Herrera, J.; Hose, J.; Hrupec, D.; Ishio, K.; Konno, Y.; Kubo, H.; Kushida, J.; Kuvež dić, D.; Lelas, D.; Lindfors, E.; Lombardi, S.; Longo, F.; López, M.; Maggio, C.; Majumdar, P.; Makariev, M.; Maneva, G.; Manganaro, M.; Mannheim, K.; Maraschi, L.; Mariotti, M.; Martínez, M.; Masuda, S.; Mazin, D.; Mielke, K.; Minev, M.; Miranda, J. M.; Mirzoyan, R.; Moralejo, A.; Moreno, V.; Moretti, E.; Nagayoshi, T.; Neustroev, V.; Niedzwiecki, A.; Nievas Rosillo, M.; Nigro, C.; Nilsson, K.; Ninci, D.; Nishijima, K.; Noda, K.; Nogués, L.; Paiano, S.; Palacio, J.; Paneque, D.; Paoletti, R.; Paredes, J. M.; Pedaletti, G.; Peresano, M.; Persic, M.; Prada Moroni, P. G.; Prandini, E.; Puljak, I.; Garcia, J. R.; Reichardt, I.; Rhode, W.; Ribó, M.; Rico, J.; Righi, C.; Rugliancich, A.; Saito, T.; Satalecka, K.; Schweizer, T.; Sitarek, J.; Šnidarić, I.; Sobczynska, D.; Stamerra, A.; Strzys, M.; Surić, T.; Takahashi, M.; Takalo, L.; Tavecchio, F.; Temnikov, P.; Terzić, T.; Teshima, M.; Torres-Albà, N.; Treves, A.; Tsujimoto, S.; Vanzo, G.; Vazquez Acosta, M.; Vovk, I.; Ward, J. E.; Will, M.; Zarić, D.; Becerra González, J.; Tanaka, Y.; Ojha, R.; Finke, J.; Lähteenmäki, A.; Järvelä, E.; Tornikoski, M.; Ramakrishnan, V.; Hovatta, T.; Jorstad, S. G.; Marscher, A. P.; Larionov, V. M.; Borman, G. A.; Grishina, T. S.; Kopatskaya, E. N.; Larionova, L. V.; Morozova, D. A.; Savchenko, S. S.; Troitskaya, Yu. V.; Troitsky, I. S.; Vasilyev, A. A.; Agudo, I.; Molina, S. N.; Casadio, C.; Gurwell, M.; Carnerero, M. I.; Protasio, C.; Acosta Pulido, J. A

Publication: *eprint arXiv:1801.04138*

Publication Date: 01/2018

Abstract: http://adsabs.harvard.edu/abs/2018arXiv180104138M

Title: Molecular Reconnaissance of the β Pictoris Gas Disk with the SMA: A Low HCN/(CO+CO2) Outgassing Ratio and Predictions for Future Surveys

Authors: Matrà, L.; Wilner, D. J.; Öberg, K. I.; Andrews, S. M.; Loomis, R. A.; Wyatt, M. C.; Dent, W. R. F.

Publication: *The Astrophysical Journal, Volume 853, Issue 2, article id. 147, 13 pp. (2018). (ApJ Homepage)*

Publication Date: 02/2018

Abstract: http://adsabs.harvard.edu/abs/2018ApJ...853..147M

Title: The Herschel-ATLAS: magnifications and physical sizes of 500-μm-selected strongly lensed galaxies

Authors: Enia, A.; Negrello, M.; Gurwell, M.; Dye, S.; Rodighiero, G.; Massardi, M.; De Zotti, G.; Franceschini, A.; Cooray, A.; van der Werf, P.; Birkinshaw, M.; Michałowski, M. J.; Oteo, I.

Publication: *Monthly Notices of the Royal Astronomical Society, Volume 475, Issue 3, p.3467-3484 (MNRAS Homepage)*

Publication Date: 04/2018

Abstract: http://adsabs.harvard.edu/abs/2018MNRAS.475.3467E

Title: On the Nature of Orion Source I

Authors: Báez-Rubio, A.; Jiménez-Serra, I.; Martín-Pintado, J.; Zhang, Q.; Curiel, S.

Publication: *The Astrophysical Journal, Volume 853, Issue 1, article id. 4, 11 pp. (2018). (ApJ Homepage)*

Publication Date: 01/2018

Abstract: http://adsabs.harvard.edu/abs/2018ApJ...853....4B

Title: High-resolution SMA imaging of bright submillimetre sources from the SCUBA-2 Cosmology Legacy Survey

Authors: Hill, Ryley; Chapman, Scott C.; Scott, Douglas; Petitpas, Glen; Smail, Ian; Chapin, Edward L.; Gurwell, Mark A.; Perry, Ryan; Blain, Andrew W.; Bremer, Malcolm N.; Chen, Chian-Chou; Dunlop, James S.; Farrah, Duncan; Fazio, Giovanni G.; Geach, James E.; Howson, Paul; Ivison, R. J.; Lacaille, Kevin; Michałowski, Michał J.; Simpson, James M.; Swinbank, A. M.; van der Werf, Paul P.; Wilner, David J.

Publication: *Monthly Notices of the Royal Astronomical Society, Volume 477, Issue 2, p.2042-2067 (MNRAS Homepage)*

Publication Date: 06/2018

Abstract: http://adsabs.harvard.edu/doi/10.1093/mnras/sty746

Title: The hypersoft state of Cygnus X-3. A key to jet quenching in X-ray binaries?
Authors: Koljonen, K. I. I.; Maccarone, T.; McCollough, M. L.; Gurwell, M.; Trushkin, S. A.; Pooley, G. G.; Piano, G.; Tavani, M.
Publication: *Astronomy & Astrophysics, Volume 612, id.A27, 15 pp. (A&A Homepage)*
Publication Date: 04/2018
Abstract: http://adsabs.harvard.edu/abs/2017arXiv171207933K

Title: Discovery of massive star formation quenching by non-thermal effects in the centre of NGC 1097
Authors: Tabatabaei, F. S.; Minguez, P.; Prieto, M. A.; Fernández-Ontiveros, J. A.
Publication: *Nature Astronomy, Volume 2, p. 83-89*
Publication Date: 01/2018
Abstract: http://adsabs.harvard.edu/abs/2018NatAs...2...83T

Title: A dusty star-forming galaxy at z = 6 revealed by strong gravitational lensing
Authors: Zavala, Jorge A.; Montaña, Alfredo; Hughes, David H.; Yun, Min S.; Ivison, R. J.; Valiante, Elisabetta; Wilner, David; Spilker, Justin; Aretxaga, Itziar; Eales, Stephen; Avila-Reese, Vladimir; Chávez, Miguel; Cooray, Asantha; Dannerbauer, Helmut; Dunlop, James S.; Dunne, Loretta; Gómez-Ruiz, Arturo I.; Michałowski, Michał J.; Narayanan, Gopal; Nayyeri, Hooshang; Oteo, Ivan; Rosa González, Daniel; Sánchez-Argüelles, David; Schloerb, F. Peter; Serjeant, Stephen; Smith, Matthew W. L.; Terlevich, Elena; Vega, Olga; Villalba, Alan; van der Werf, Paul; Wilson, Grant W.; Zeballos, Milagros
Publication: *Nature Astronomy, Volume 2, p. 56-62*
Publication Date: 01/2018
Abstract: http://adsabs.harvard.edu/abs/2017arXiv170709022Z

The Submillimeter Array (SMA) is a pioneering radio-interferometer dedicated to a broad range of astronomical studies including finding protostellar disks and outflows; evolved stars; the Galactic Center and AGN; normal and luminous galaxies; and the solar system. Located on Maunakea, Hawaii, the SMA is a collaboration between the Smithsonian Astrophysical Observatory and the Academia Sinica Institute of Astronomy and Astrophysics.

SUBMILLIMETER ARRAY
Harvard-Smithsonian Center
for Astrophysics
60 Garden Street, MS 78
Cambridge, MA 02138 USA
www.cfa.harvard.edu/sma/

SMA HILO OFFICE
645 North A'ohoku Place
Hilo, Hawaii 96720
Ph. 808.961.2920
Fx. 808.961.2921
sma1.sma.hawaii.edu

ACADEMIA SINICA INSTITUTE OF
ASTRONOMY & ASTROPHYSICS
P.O. Box 23-141
Taipei 10617
Taiwan R.O.C.
www.asiaa.sinica.edu.tw/